168296

SOLUTIONS OF THE NAVIER-STOKES EQUATIONS AND TECHNOLOGICAL APPLICATIONS USING MATRIX-DISTRIBUTION WITH N-METHODS

by
EYLEM GÜLCE ÇOKER

Submitted to the Institute of Graduate Studies in
Science and Engineering in partial fulfillment of
the requirements for the degree of
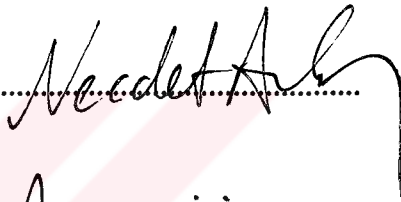Master of Science
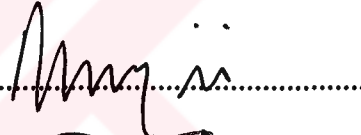in
Physics

Yeditepe University

2005

SOLUTIONS OF THE NAVIER-STOKES EQUATIONS AND TECHNOLOGICAL
APPLICATIONS USING MATRIX-DISTRIBUTION WITH N-METHODS

APPROVED BY:

Prof. Dr. Necdet ASLAN
(Thesis Supervisor)

Prof. Dr. Ahmet T. İNCE

Assoc. Prof. Dr. Şahin AKTAŞ

DATE OF APPROVAL: 31.05.2005

ACKNOWLEDGEMENTS

ABSTRACT

SOLUTIONS OF THE NAVIER-STOKES EQUATIONS AND TECHNOLOGICAL APPLICATIONS USING MATRIX-DISTRIBUTION WITH N-METHODS

The interaction of an externally imposed magnetic and electric field on the laminar flow of a conducting fluid in a channel is studied using computational techniques. The Navier-Stokes (N-S) equations and the equations describing the electromagnetic field (MHD) are solved simultaneously in a computational fluid dynamics code that utilizes a matrix distribution scheme. The flow considered is two-dimensional on x-y plane. The MHD flow includes an imposed electric and magnetic field acting also on this plane along the central region of the channel and activated by a switch at a specified time (after the vertical flow reaches steady state). A magnet is placed on both sides of the channel and an external magnetic field configuration is obtained in the direction connecting the left and right walls. In addition, an external electric field is applied in perpendicular direction such that **ExB** becomes opposite to gravitational acceleration direction. This is done to slow down (or even control) the vertical velocity in the channel. The calculations are done with a new solver using a matrix distribution scheme that works on structured and unstructured triangular meshes. The N-S and MHD equations are first written in nondimensional forms and the numerical scheme was obtained. For time iterations , a 3-stage Runga-kutta method is used. The numerical results show that this computer code is capable of resolving different types of problems in different geometries.

ÖZET

NAVIER-STOKES DENKLEMLERİNİN MATRİS DAĞILIMI VE N METODU İLE NUMERİK ÇÖZÜMLERİ VE TEKNOLOJİK UYGULAMALARI

Dış elektrik ve manyetik alanların kanallarda akan iletken akışkanlara etkisi nümerik tekniklerle incelenmiştir. Hidrodinamiği, N-S ve elektromanyetik alanları tanımlayan Maxwell denklemleri, matris dağılımı metodu ile birlikte Magneto Hidrodinamik Denklemler (MHD) çözülmüştür. MHD akışı dik bir kanalda ortadaki bölgede bir anahtarla aniden devreye giren dış elektrik ve manyetik alan içermektedir. Kanalın iki tarafına yerleştirilen magnet ile soldan sağa duvara doğru yönelen dış manyetik alan uygulanmıştır. Ayrıca bu düzleme dik (+z) yönünde ExB yerçekimine dik olacak şekilde bir dış elektrik alan uygulanmıştır. Bunun nedeni, düşey hızı yavaşlatmak ve hatta kontrol edebilmektir. Sonuçlar, bunun bazı elektrik alan şiddetlerinde mümkün olduğunu göstermektedir.

Hesaplamalar, düzenli ve düzensiz ızgaralar için çözen yeni bir bilgisayar kodu ile yapılmıştır. N-S ve MHD denklemleri ilk önce boyutsuz hale getirilmiş ve numerik durum elde edilmiştir. Zaman iterasyonları için üç kademeli Runga-Kutta metodu kullanılmıştır. Elde edilen sonuçlar geliştirilen bu kodun birçok problemi rahatlıkla çözebilecek kapasitede olduğunu göstermektedir.

TABLE OF CONTENTS

LIST OF FIGURES

LIST OF TABLES

LIST OF SYMBOLS

V : Velocity

R : Reynold's number

R_m : Magnetic Reynold's number

L : Length

v : Kinematic viscosity

$\rho_{m\alpha}$: Mass density

$\rho_{q\alpha}$: Charge density

Ω : Volume

m : Mass

T : Temperature

P : Pressure

R : Universal gas constant

μ : Coefficient of viscosity

n : Density

k : Boltzmann's constant

B : Magnetic field

E : Electric field

r, x : Position

t : Time

f_α : One-body distribution function

$\overline{n_\alpha}$: Number density

α : Species

V_α : Velocity of particles of species α

J_α : Current density

H_α : Heat flux

P_α : Pressure tensor

p_α : Scalar pressure

$v_{\alpha\beta}$: Collision frequency for momentum transfer

∇ : Del operator

η : Resistivity

σ : Conductivity

λ_D : Debye length

m_e : Mass of electron

m_i : Mass of ion

ω : Frequency

1. INTRODUCTION

The fluid mechanics and plasma physics engineering are two main research fields which are crucial in understanding the nature of the particle motions under the effects of internal or external forces. These fields are so important that by carefully examining the motion of the gases or liquids under the effects of internal or external fields, important simulated and then manufactured. Writing the conservation equations for all the constituents (i.e., atoms or molecules) in the system is impossible because of the requirement of huge number of equations. That's why, fluid mechanics can be used as a tool in order to understand the gross behavior of collectively moving particles. If all the properties of fluids and how these properties affect the fluid's motion are known, the flow behavior can be realized. In this thesis, we will first define and classify fluids and discuss their properties. This will be done in a systematical way by deriving the conservation laws from the kinetic formulation (i.e., Boltzmann equation: an equation describing the behavior of the particle distribution function). It will be shown that the moments of Boltzmann equation lead to the conservation of mass, momentum, and energy in order to describe hydrdynamics behavior. If the fluid particles can carry charged, Maxwell's equations must accompany these conservation laws giving rise to magneto-hydrodynamics (MHD) equations. This thesis deals with the regular fluid hydrodynamics described by Navier-Stokes (NS) equations and the MHD in which the motions are affected from electric and magnetic fields.

A fundamental problem of fluid engineering is to predict the aerodynamic forces, moments and the heat-transfer rates during the fluid motion within an enclosed volume or around vehicles or obstacles. In order to predict these aerodynamic forces and moments with reasonable accuracy, it is necessary to be able to describe the flow pattern in the medium. The resultant flow pattern depends on the geometry of the medium or the vehicle, their orientation with respect to the undisturbed free stream, altitude and speed at which the fluid or vehicle is traveling. In analyzing the various flows that the fluid engineers may encounter, some assumptions about the fluid or medium properties should be introduced. In some applications, the temperature variations are so small that they do not affect the

velocity field. In addition, for those applications where the temperature variations have a negligible effect on the flow field, it is often assumed that the density is essentially constant.

However, in analyzing high-speed flows, the density variations cannot be neglected. In that case, the density may be expressed in terms of pressure and temperature. In fact, for a gas in thermodynamic equilibrium, any thermodynamic property may be expressed as a function of two other independent, thermodynamic properties. Thus, it is possible to formulate the governing equations using the enthalpy and the entropy as the flow properties instead of the pressure and the temperature. In this thesis, incompressible low-speed flows are considered so that constant density cases are considered. From the point of view of fluid mechanics, matter can be in one of two states, either solid or fluid. The technical distinction between these two states lies in their response to an applied shear, or tangential, stress. A solid can resist a shear stress by a static deformation; a fluid cannot. A fluid is a substance that deforms continuously under the action of shearing forces. An important corollary of this definition is that there can be no shear stresses acting on fluid particles if there is no relative motion within the fluid; that is, such fluid particles are not deformed. Thus, if the fluid particles are at rest or if they are all moving at the same velocity, there are no shear stresses in the fluid. This zero shear stress condition is known as the hydrostatic stress condition.

In problems of interest to this thesis, our primary concern is not with the motion of individual molecules, but with the general behavior of the fluid. Thus, we are concerned with describing the fluid motion in spaces that are very large compared to molecular dimensions and that, therefore, contain a large number of molecules. The fluid in these problems may be considered to be a continuous material whose properties can be determined from a statistical average for the particles in the volume, that is, a macroscopic representation. The assumption of a continuous fluid is valid when the smallest volume of fluid that is of interest contains so many molecules that statistical averages are meaningful. In this thesis the properties of fluids which are the temperature, the pressure, the density, and the viscosity are explained in detail.

The plasma will be explained in the third section of this thesis. A meaningful definition will be given as in Ref.[1]. Also we will see the applications of plasma physics in this section. On the other hand we will look at the macroscopic properties of plasma where we will be able to find the distribution function. As already known the moments of the distribution function gives us the continuity equations which are the basic equations for us to solve the magneto-hydrodynamic equations.

Basic conservation laws and the effects of them on Navier-Stokes and MHD equations will be shown on the fifth section. The aim of this section is to derive the set of equations which results from the physical laws of conservation of mass, momentum, and energy. First of all, the statistical and the continuum methods will be explained to derive the conservation laws. Then, the Eulerian and the Lagrangian coordinates will be employed which are the two basic coordinate systems to formulate the conservation laws. In the Eulerian framework the independent variables are the spatial coordinates x,y,z, and time t. Most of the problems are solved in this framework. The attention is focused on the fluid which passes through a control volume which is fixed in space; whereas, in the Lagrangian approach, attention is fixed on a particular mass of fluid as it flows. This will be explained more detailly in the fifth section.

The mathematical model of any fundamental fluid dynamics problem is governed by the Navier-Stokes equations. These equations are important and represent the fluid as a continuum. The equations conserve mass, momentum, and energy, and can be derived either an integral or a differential approach. The integral form of the equations is derived using Reynolds Transport Theorem (RTT). [2], [3]. The approach we follow in this thesis is given briefly in section six.

The definition of magnetohydrodynamics (MHD) which is used in this thesis, is, when a conducting fluid or an ionized gas, a plasma, moves in a magnetic field an electric field is produced and an electric current appears. In turn, the interaction of the current with the magnetic field changes the motion of the fluid and changes the magnetic field. Magnetohydrodynamics is that part of the mechanics of continuous media which studies

the motion of electrically conducting media in the presence of a magnetic field. [4]. In other words, magnetohydrodynamics studies the physics of fluid, or gaseous conductors in a magnetic field. Apart from this definition, in which the subject of the studies is indicated, but not the approximation which is applied (MHD in the wider sense), one understands by magnetohydrodynamics the low-frequency limit when one neglects not only kinetic effects, which occur due to the thermal spread of the particles, but also the difference in motion of the various kinds of ions, and neutral particles. [5]

In this thesis, we studied with the incompressible fluids which is described in detail in the next paragraph.

The Navier-Stokes equations simplify considerably for incompressible fluids for which the specific mass may be considered as constant. This leads generally to a separation of the energy equation from the other conservation laws if the flow remains isothermal. This is the case for many applications which do not involve heat transfer.

For flows involving temperature variations the coupling between the temperature field and the fluid motion can occur through various effects, such as variations of viscosity or heat conductivity with temperature; the influence of external forces as a function of temperature (for example, buoyancy forces in atmospheric flows); and electrically, mechanically or chemically generated heat sources.

In the case of incompressible flows the mass conservation equation reduces to $\nabla \cdot \mathbf{V} = 0$ which appears as a kind of constraint to the general time-dependent equation of motion.

For incompressible flows, an alternative formulation can be obtained through the Helmholtz vorticity .

If no density stratification is to be considered the contribution of the pressure term disappears completely from the vorticity equation. Moreover, for plane two-dimensional flows the first term of the right-hand side vanishes. The system of equations for incompressible flow presents a particular situation in which one of the five unknowns, namely the pressure, does not appear under a time-dependence form due to the non-

evolutionary character of the continuity equation. This actually creates a difficult situation for the numerical schemes and special techniques have to be adapted in order to treat the continuity equation. For more details we refer the reader to the corresponding sections of the thesis.An equation for the pressure can be obtained by taking the divergence of the momentum equation which can be considered as a Poisson equation for the pressure for a given velocity field.

For laminar, incompressible, isothermal flows no additional input is necessary to. solve the system of flow equations besides the value of the fluid constant p. Therefore it can be considered that the domain of laminar flows can be completely described for any set of initial and boundary conditions by computation, without having to resort to additional empirical information. Today, this phase can be considered to be close to realization, even for three-dimensional flow situations at reasonable computer times.

Direct simulation for large-scale coherent structures. The numerical simulation of vortex shedding behind bluff bodies is of importance in view of applications such as atmospheric flows around buildings, vehicle aerodynamics or combustor flows. An impressive example of computation of the vortex shedding created by the flow around a square cylinder has been reported by Davis et al (1984). The calculated flow field with a visualization under similar conditions in a wind tunnel at a Reynolds number of $Re = 550$. An illustration of a similar computation by these authors of an unstable mixing layer compared with visualization under the same conditions.

These results emphasize the stage achieved nowadays in the numerical computation of complex flow fields via the resolution of Navier-Stokes equations. Although, as can be seen from the above results, many aspects of the flow can be reproduced, they are still to be considered as first approximations, since these computations are two-dimensional and do not contain the effect of the small-scale turbulence.

The system of Navier-Stokes equations is indeed valid for the laminar flow of a viscous, Newtonian fluid. In reality, the flow will remain laminar up to a certain critical value of the Reynolds number $V \cdot L/v$, where V and L are representative values of velocity and length scales for the considered flow system. Above this critical value the flow becomes turbulent and is characterized by the appearance of fluctuations of all the

variables (velocity, pressure, density, temperature, etc.) around mean values. These fluctuations are of a statistical nature and hence cannot be described in a deterministic way. However, they could be computed numerically in direct simulations of turbulence, such as the 'large eddy simulation' approach, whereby only the small-scale turbulent fluctuations are modeled and the larger-scale fluctuations are computed directly. The reader can find a review of the state of the art of direct numerical simulation of turbulence in Rogallo and Moin (1984) and Moin (1984). Although this approach requires considerable computer resources, it has already led to very encouraging results.

At present these approaches are still far from being applicable for practical calculations in industrial environments, due to the considerable requirements they put on computational resources. There is no doubt, however, that these methods will become increasingly important in the future, since they require the lowest possible amount of external information in addition to the basic Navier-Stokes equations.

2. THE PROPERTIES OF FLUIDS

From the point of view of fluid mechanics, matter can be in one of two states, either solid or fluid. The technical distinction between these two states lies in their response to an applied shear, or tangential, stress. A solid can resist a shear stress by a static deformation; a fluid cannot. A fluid is a substance that deforms continuously under the action of shearing forces. An important corollary of this definition is that there can be no shear stresses acting on fluid particles if there is no relative motion within the fluid; that is, such fluid particles are not deformed. Thus, if the fluid particles are at rest or if they are all moving at the same velocity, there are no shear stresses in the fluid. This zero shear stress condition is known as the hydrostatic stress condition.

A fluid can be either a liquid or a gas. A liquid is composed of relatively close packed molecules with strong cohesive forces. As a result, a given mass of liquid will occupy a definite volume of space. If a liquid is poured into a container, it assumes the shape of the container up to the volume it occupies and will form a free surface in a gravitational field if unconfined from above. The upper (or free) surface is planar and perpendicular to the direction of gravity. Gas molecules are widely spaced with relatively small cohesive forces. Therefore, if a gas is placed in a closed container, it will expand until it fills the entire volume of the container. A gas has no definite volume. Thus, if it is unconfined, it forms an atmosphere that is essentially hydrostatic.

2.1. Fluid As A Continuum

When developing equations to describe the motion of a system of fluid particles, one can either define the motion of each and every molecule or one can define the average behavior of the molecules within a given control volume. The size of the control volume is important, but only in relation to the number of fluid particles contained in the volume and to the physical dimensions of the flow field. Thus, the control volume should be large compared with the volume occupied by a single molecule so that it contains a large number of molecules at any instant of time. Furthermore, the number of molecules within the volume will remain essentially constant even though there is a continuous flux of

molecules through the boundaries. If the control volume is too large, there could be a noticeable variation in the fluid properties determined statistically at various points in the volume.

In problems of interest to this thesis, our primary concern is not with the motion of individual molecules, but with the general behavior of the fluid. Thus, we are concerned with describing the fluid motion in spaces that are very large compared to molecular dimensions and that, therefore, contain a large number of molecules. The fluid in these problems may be considered to be a continuous material whose properties can be determined from a statistical average for the particles in the volume, that is, a macroscopic representation. The assumption of a continuous fluid is valid when the smallest volume of fluid that is of interest contains so many molecules that statistical averages are meaningful.

The number of molecules in a cubic meter of air at room temperature and at sea-level pressure is approximately 2.5×10^{25}. Thus, there are 2.5×10^{10} molecules in a cube 0.01 mm on a side. The mean free path at sea level is 6.6×10^{-8} m. There are sufficient molecules in this volume for the fluid to be considered a continuum, and the fluid properties can be determined from statistical averages. However, at an altitude of 130 km, there are only 1.6×10^{17} molecules in a cube 1 m on a side. The mean free path at this altitude is 10.2 m. Thus, at this altitude the fluid cannot be considered a continuum.

2.2. Fluid Properties

By employing the concept of a continuum, we can describe the gross behavior of the fluid motion using certain observable, macroscopic properties. Properties used to describe a general fluid motion include the temperature, the pressure, the density, and the viscosity.

2.2.1. Temperature

We are all familiar with temperature in qualitative terms; that is, an object feels hot (or cold) if it is touched. However, because of the difficulty in quantitatively defining the temperature, we define the equality of temperature. Two bodies that are in thermal contact have equal temperature when no observable property changes. Statistically, the number of possible states is related to the energy of the particles. The temperature is a quantity which shows how the number of states changes with energy changes.

2.2.2. Pressure

Because of the random motion due to their thermal energy, the individual molecules of a fluid would continually strike a surface that is placed in the fluid. These collisions occur even though the surface is at rest relative to the fluid. By Newton's second law, a force is exerted on the surface equal to the time rate of change of the momentum of the rebounding molecules. *Pressure* is the magnitude of this force per unit area of surface. Since a fluid that is at rest cannot sustain tangential forces, the pressure on the surface must act in the direction perpendicular to that surface. Furthermore, the pressure acting at a point in a fluid at rest is the same in all directions. *Standard atmospheric pressure* is defined as the pressure that can support a column of mercury 760 mm in length when the density of the mercury is 13.5951 g/cm^3 and the acceleration due to gravity is the standard value. The standard atmospheric pressure is 1.01325×10^5 N/m^2. In many fluid flow applications, the difference between the local pressure and the atmospheric pressure is utilized. Many pressure gages indicate the difference between the absolute pressure and the atmospheric pressure existing at the gage. In this thesis, the pressure differences will be utilized in deriving a physically meaningful dimensionless momentum equation.

2.2.3. Density

The *density* of a fluid at a point in space is the mass of the fluid per unit volume surrounding the point. As is the case when evaluating the other fluid properties, the incremental volume must be large compared to molecular dimensions but smaller than the

size of the system. Thus, provided that the fluid may be assumed to be a continuum, the density at a point is defined as:

$$\rho = \lim_{\delta\Omega\to 0} \frac{\delta m}{\delta\Omega} \qquad (2.1)$$

where m is the mass, Ω is the volume. In general, the density of a gas is a function of the composition of the gas, its temperature T, and its pressure P, the relation

$$\rho \, (composition, T, P) \qquad (2.2)$$

is known as an equation of state. For a thermally perfect gas, the equation of state is

$$\rho = \frac{P}{RT} \qquad (2.3)$$

where ρ is the density, P is the pressure, T is the temperature, and R is the gas constant which has a particular value for each substance. The gas constant for air has the value 287.05 N.m/kg .K in SI units. The temperature in Equation (2.3) should be in absolute units. Thus, the temperature is in K but never in °C. For the fluid flows at approximately 100 m/s, or less, the density of the air flowing is assumed constant when obtaining a solution for the flow field. Rigorous application of Equation (2.3) would require that the pressure and the temperature remain constant (or change proportionally) in order for the density to remain constant throughout the flow field. The assumption of constant density for velocities below 100 m/s is a valid approximation because the pressure changes that occur from one point to another in the flow field are small relative to the absolute value of the pressure. In this thesis, slow motions are considered such that the density remains constant at all times and that the flows that are investigated display incompressible behavior.

2.2.4. Viscosity

In all real fluids, a shearing deformation is accompanied by a shearing stress. The fluids of interest in this thesis are Newtonian in nature; that is, the shearing stress is

proportional to the rate shearing deformation. The constant of proportionality is called the *coefficient of viscosity*, μ .Thus,

$$\text{shear stress} = \mu \; . \; (\text{transverse gradient of velocity}) \qquad (2.4)$$

Being a transport property, viscosity of a fluid relates to the transport of momentum in the direction of the velocity gradient (but opposite in sense). In general, the coefficient of viscosity is a function of the composition of the gas, its temperature, and its pressure. For temperatures below 3000 K, the viscosity of air is independent of pressure. In this temperature range, we could use Sutherland's equation to calculate the coefficient of viscosity[3]:

$$\mu = 1.458 \times 10^{-6} \frac{T^{1.5}}{T + 110.4} \qquad (2.5)$$

where T is the temperature in K and the units for μ are kg/s . m.

Equations used to calculate the coefficient of viscosity depend on the model used to describe the intermolecular forces of the gas molecules, so that it is necessary to define the potential energy of the interaction of the colliding molecules. It is noted that the potential for the Sutherland model is described physically as a rigid, impenetrable sphere, surrounded by an inverse-power attractive force. This model is qualitatively correct in that the molecules attract one another when they are far apart and exert strong repulsive forces upon one another when they are close together.

Equation (2.5) closely represents the variation of μ with temperature over a "fairly" wide range of temperatures. They caution, however, that the success of Sutherland's equation in representing the variation of μ with temperature for several gases does not establish the validity of Sutherland's molecular model for those gases. "In general it is not adequate to represent the core of a molecule as a rigid sphere, or to take molecular attractions into account to a first order only. The greater rapidity of the experimental increase of μ with T, as compared with that for non-attracting rigid spheres, has to be explained as due partly to the 'softness' of the repulsive field at small distances and partly to

attractive forces which have more than a first-order effect. The chief value of Sutherland's formula seems to be as a simple interpolation formula over restricted ranges of temperature."

The Lennard-Jones model for the potential energy of an interaction, which takes into account both the softness of the molecules and their mutual attraction at large distances, has been used [8] to calculate the viscosity and the thermal conductivity of gases at high temperatures. The coefficients of viscosity for air as tabulated by Svehla are compared with the values calculated using Equation (2.5) in Table 2.1. These comments are made to emphasize the fact that even the basic fluid properties may involve approximate models that have a limited range of applicability.

Table 2.1 Comparison of the coefficient of viscosity for air as tabulated [8] and as calculated using Sutherland's equation, Equation (2.5).

T (K)	$\dfrac{\mu}{10^5}$ (kg/m-s) Ref[?]	$\mu \times 10^5$ (kg/m-s) Equation (2.5)
20	1.36	1.329
40	2.27	2.285
60	2.99	3.016
80	3.61	3.624
100	4.17	4.152
120	4.69	4.625
140	5.19	5.057
160	5.67	5.456
180	6.12	5.828
200	6.55	6.179
220	6.97	6.512
240	7.37	6.829

2.2.5. Kinematic Viscosity

The fluid engineer may encounter many applications where the ratio μ/ρ has been replaced by a single parameter. Because this ratio appears frequently, it has been given a special name, the kinematic viscosity. The symbol used to represent the kinematic viscosity is ν:

$$\nu = \frac{\mu}{\rho} \tag{2.6}$$

In this ratio, the force units (or, equivalently, the mass units) cancel. Thus, ν has the dimensions of L^2/T.

3. THE DEFINITION OF PLASMA

It is often said that 99% of the matter in the universe is in the plasma state; that is, in the form of an electrified gas with the atoms dissociated into positive ions and negative electrons. This estimate may not be very accurate, but it is certainly a reasonable one in view of the fact that stellar interiors and atmospheres, gaseous nebulae, and much of the interstellar hydrogen are plasmas. In our own neighbourhood, as soon as one leaves the earth's atmosphere, one encounters the plasma comprising the Van Allen radiation belts and the solar wind. On the other hand, in our everyday lives encounters with plasmas are not limited to a few examples: the flash of a lightning bolt, the soft glow of the Aurora Borealis, the conducting gas inside a fluorescent tube or neon sign, and the slight amount of ionization in a rocket exhaust. Any ionized gas cannot be called a plasma, of course; there is always some small degree of ionization in any gas. A useful definition is as follows:

A plasma is a quasineutral gas of charged and neutral particles which exhibits collective behavior. [1]

Consider the forces acting on a molecule of ordinary air. Since the molecule is neutral, there is no net electromagnetic force on it, and the force of gravity is negligible.

The molecule moves undisturbed until it makes a collision with another molecule, and these collisions control the particle's motion. A macroscopic force applied to a neutral gas, such as from a loudspeaker generating sound waves, is transmitted to the individual atoms by collisions. The situation is totally different in a plasma, which has charged particles. As these charges move around, they can generate local concentrations of positive or negative charge, which give rise to electric fields. Motion of charges also generates currents, and hence magnetic fields. These fields affect the motion of other charged particles far away.

Let us consider the effect on each other two slightly charged regions of plasma separated by a distance r (Fig.3.1). The Coulomb force between A and B diminishes as $1/r^2$. However, for a given solid angle (that is, $\Delta r / r = constant$), the volume of plasma in B that can affect A increases as r^3.
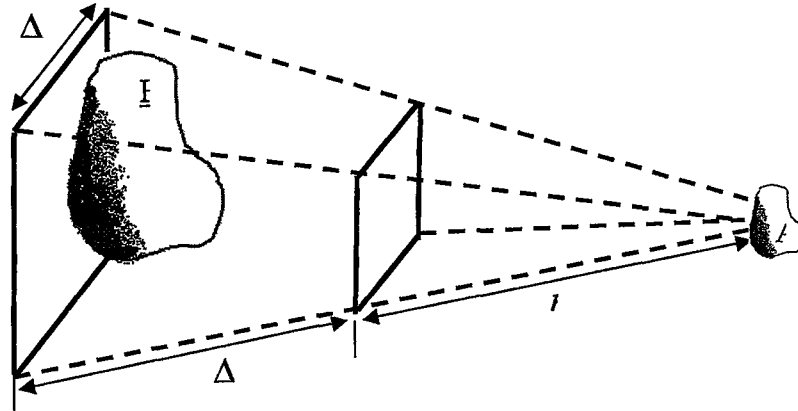
Figure 3.1. The long range of electrostatic forces in a plasma

Therefore, elements of plasma exert a force on one another even at large distances. It is this long-ranged Coulomb force that gives the plasma a large repertoire of possible motions and enriches the field of study known as plasma physics. In fact, the most interesting results concern so-called 'collisionless' plasmas, in which the long-range electromagnetic forces are so much larger than the forces due to ordinary local collisions that the latter can be neglected altogether. By 'collective behavior' we mean motions that depend not only on local conditions but on the state of the plasma in remote regions as well.

3.1 Applications of Plasma Physics

Plasmas can be characterized by the two parameters n and kT_e. Plasma applications cover an extremely wide range of n and kT_e: n varies over 28 orders of magnitude from 10^6 to 10^{34} m^{-3}, and kT can vary over seven orders from 0.1 to 10^6 eV. Some of these applications are discussed very briefly below. The tremendous range of density can be appreciated when one realizes that air and water differ in density by only 10^3, while water and white dwarf stars are separated by only a factor of 10^5. Even neutron stars are only 10 times denser than water. Yet gaseous plasmas in the entire density range of 10^{28} can be

described by the same set of equations, since only the classical (non-quantum mechanical) laws of physics are needed.

3.1.1. Gas Discharges (Gaseous Electronics)

The earliest work with plasmas was that of Langmuir, Tonks, and their collaborators in the 1920's. This research was inspired by the need to develop vacuum tubes that could carry large currents, and therefore had to be filled with ionized gases. The research was done with weakly ionized glow discharges and positive columns typically with $kT_e \cong 2$ eV and $10^{14} < n < 10^{18} \, m^{-3}$. It was here that the shielding phenomenon was discovered; the sheath surrounding an electrode could be seen visually as a dark layer. Gas discharges are encountered nowadays in mercury rectifiers, hydrogen thyratrons, ignitrons, spark gaps, welding arcs, neon and fluorescent lights, and lightning discharges. Thus, understanding the behavior of the gas discharges is crucial in the development of such high-tech equipments.

3.1.2. Controlled Thermonuclear Fusion

Modern plasma physics had it beginnings around 1952, when it was proposed that the hydrogen bomb fusion reaction be controlled to make a reactor. The principal reactions, which involve deuterium (D) and tritium (T) atoms, are as follows:

$$D + D \rightarrow {}^3He + n + 3.2\text{MeV}$$

$$D + D \rightarrow T + p + 4.0\text{MeV}$$

$$D + T \rightarrow {}^3He + n + 17.6\text{MeV}$$
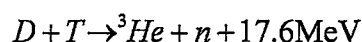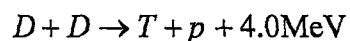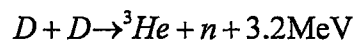
The cross sections for these fusion reactions are appreciable only for incident energies of D or T above 5 keV (extremely hot). Accelerated beams of deuterons bombarding a target will not work, because most of the deuterons will lose their energy by scattering before undergoing a fusion reaction. It is necessary to create a plasma in which the thermal energies are in the 10-keV range. The problem of heating and containing such a

plasma is responsible for the rapid growth of the science of plasma physics since 1952. The problem is not totally solved, and most of the active research in plasma physics is directed toward the solution of this problem.

3.1.3. Space Physics

Another important application of plasma physics is in the study of the earth's environment in space. A continuous stream of charged particles, called the solar wind, impinges on the earth's magnetosphere, which shields us from this radiation and is distorted by it in the process. Typical parameters in the solar wind are $n = 5 \times 10^6$ m^{-3}, $kT_i = 10$ eV, $kT_e = 50$ eV, $B = 5 \times 10^{-9}$T, and drift velocity 300 km/sec. The ionosphere, extending from an altitude of 50 km to 10 earth radii, is populated by a weakly ionized plasma with density varying with altitude up to $n = 10^{12}$ m^{-3}. The temperature is only 10^{-1} eV. The Van Allen belts are composed of charged particles trapped by the earth's magnetic field. Here we have $n < 10^9$ m^{-3}, $kT_e < 1$ keV, $kT_i - 1$ eV, and $B \cong 500 \times 10^{-9}$T.

3.1.4. Modern Astrophysics

Stellar interiors and atmospheres are hot enough to be in the plasma state. The temperature at the core of the sun, for instance, is estimated to be 2 keV; thermonuclear reactions occurring at this temperature are responsible for the sun's radiation. The solar corona is a tenuous plasma with temperatures up to 200 eV. The interstellar medium contains ionized hydrogen with $n \cong 10^6$ m^{-3}. Various plasma theories have been used to explain the acceleration of cosmic rays. Although the stars in a galaxy are not charged, they behave like particles in a plasma; and plasma kinetic theory has been used to predict the development of galaxies. Radio astronomy has uncovered numerous sources of radiation that most likely originate from plasmas. The Crab nebula is a rich source of plasma phenomena because it; is known to contain a magnetic field. It also contains a visual pulsar. Current theories of pulsars picture them as rapidly rotating neutron stars with plasmas emitting synchrotron radiation from the surface.

3.1.5. MHD Energy Conversion and Ion Propulsion

Getting back down to earth, we come to two practical applications of plasma physics. MHD energy conversion utilizes a dense plasma jet propelled across a magnetic field to generate electricity Figure 3.2.
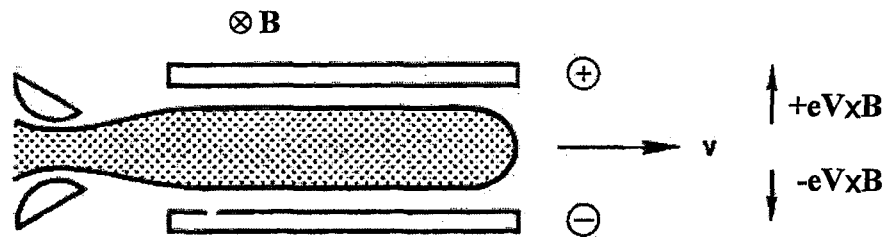
Figure 3.2. Principle of the MHD generator.

The Lorentz force $q\mathbf{v} \times \mathbf{B}$, where $\mathbf{v}$ is the jet velocity, causes the ions to drift upward and the electrons downward, charging the two electrodes to different potentials. Electrical current can the be drawn from the electrodes without the inefficiency of a heat cycle.

The same principle in reverse has been used to develop engines for interplanetary missions. In Figure 3.3, a current is driven through a plasma by applying a voltage to the two electrodes. The $\mathbf{j} \times \mathbf{B}$ force shoots the plasma out of the rocket, and the ensuing reaction force accelerates the rocket. The plasma ejected must always be neutral; otherwise, the space ship will be charged to a high potential.
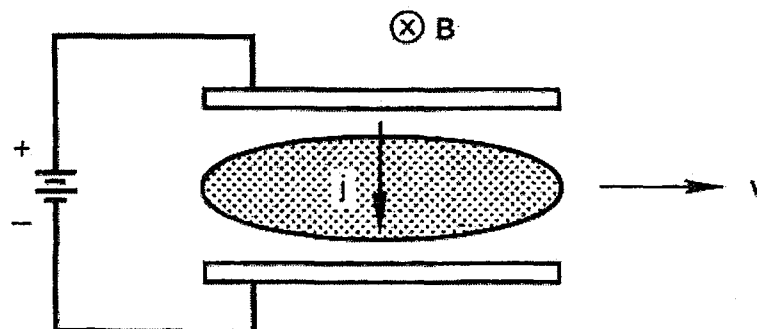
Figure 3.3. Principle of plasma-jet engine for spacecraft propulsion.

3.1.6. Solid State Plasmas

The free electrons and holes in semiconductors constitute a plasma exhibiting the same sort of oscillations and instabilities as a gaseous (plasma. Plasmas injected into InSb have been particularly useful in studies of these phenomena. Because of the lattice effects, the effective collision frequency is much less than one would expect in a solid with $n \cong 10^{29}$ m^{-3}. Furthermore, the holes in a semiconductor can have a very low effective mass—as little as 0.01 m_e—and therefore have high cyclotron frequencies even in moderate magnetic fields. If one were to calculate N_D for a solid state plasma, it would be less than unity because of the low temperature and high density. Quantum mechanical effects (uncertainty principle), however, give the plasma an effective temperature high enough to make N_D respectably large. Certain liquids, such as solutions of sodium in ammonia, have been found to behave like plasmas also.

3.1.7. Gas Lasers

The most common method to "pump" a gas laser—that is, to invert the population in the states that give rise to light amplification—is to use a gas discharge. This can be a low-pressure glow discharge for a dc laser or a high-pressure avalanche discharge in a pulsed laser. The He-Ne lasers commonly used for alignment and surveying and the Ar and Kr lasers used in light shows are examples of dc gas lasers. The powerful CO_2 laser is finding commercial application as a cutting tool. Molecular lasers make possible studies of the hitherto inaccessible far infrared region of the electromagnetic spectrum. These can be directly excited by an electrical discharge, as in the hydrogen cyanide (HCN) laser, or can be optically pumped by a CO_2 laser, as with the methyl fluoride (CH_3F) or methyl alcohol (CH_3OH) lasers. Even solid state lasers, such as Nd-glass, depend on a plasma for their operation, since the flash tubes used for pumping contain gas discharges.

4. MACROSCOPIC PROPERTIES OF PLASMAS

Although an exact knowledge of the state of a many-body system requires that the position and velocity of all the particles in the system be known, much of the behavior of such a system can be described in terms of macroscopic variables such as the density, the temperature, the average velocity, and the pressure. These quantities are related through the conservation laws and through the dynamical equations for momentum and energy transport. The purpose of this thesis is to define these variables and their relationships, starting from an exact many-body description, and then solve these equations to illustrate some macroscopic properties of plasmas. These variables and equations are a reduced description of the plasma, i.e., they contain less information than the complete many-body description. Therefore there are some plasma properties they cannot describe (for example, Landau damping and velocity-space instabilities). However, they are sufficient to describe a wide variety of plasma effects and applications.

The macroscopic variables for a plasma are defined in terms of velocity moments of the distribution function $f(\mathbf{r},\mathbf{v},t)$, which containes the statistical description of the system. The relationships between these macroscopic variables are derived from the differential equation for the distribution function.

4.1. Macroscopic Variables of a Plasma

The one-body distribution is a reduced description of the plasma state; however, it is not a macroscopic observable of either a plasma or neutral gas. The macroscopically observable quantities are found from the velocity moments of the one-body distribution function.

4.1.1 Density

The number of particles of species α at point $\mathbf{r}$ confined in the volume in configuration space (i.e., $\mathbf{r}$-$\mathbf{v}$ space) at time t is given by

$$n_\alpha(r,t) = \int \bar{n}_\alpha f_\alpha(r,v,t) d^3 v \qquad (4.1)$$

where f_α is the one-body distribution function (4.1), and $\bar{n}_\alpha = N_\alpha / \Omega$ is the number density. The mass density $\rho_{m\alpha}$ and the charge density $\rho_{q\alpha}$ are similarly defined; i.e.,

$$\rho_{m\alpha}(r,t) = \bar{n}_\alpha m_\alpha \int f_\alpha(r,v,t) d^3 v \qquad (4.2)$$

$$\rho_{q\alpha}(r,t) = \bar{n}_\alpha q_\alpha \int f_\alpha(r,v,t) d^3 v \qquad (4.3)$$

4.1.2. Particle Flux and Velocity

The flux of particles of species α crossing a unit area in configuration space per unit time at the point x and at time t is

$$\Gamma_\alpha(r,t) = \bar{n}_\alpha \int v f_\alpha(r,v,t) d^3 v = n_\alpha(r,t) V_\alpha(r,t) \qquad (4.4)$$

where V_α is the average velocity of particles of species α defined by

$$V_\alpha(r,t) = \frac{\int v f_\alpha(r,v,t) d^3 v}{\int f_\alpha(r,v,t) d^3 v} = \frac{\bar{n}_\alpha}{n_\alpha(r,t)} \int v f_\alpha(r,v,t) d^3 v \qquad (4.5)$$

4.1.3. Current Density

The electric current density for charged particles of species α at the point r in configuration space at time t is

$$J_\alpha(r,t) = q_\alpha \bar{n}_\alpha \int v f_\alpha d^3 v = q_\alpha \Gamma_\alpha(r,t) = q_\alpha n_\alpha(r,t) v_\alpha(r,t) \qquad (4.6)$$

4.1.4. Heat Flux

The flux of kinetic energy for particles of species α crossing a unit area in configuration space per unit time at the point $\mathbf{r}$ and at time t is

$$\mathbf{H}_\alpha(\mathbf{r},t) = \frac{1}{2}\bar{n}_\alpha m_\alpha \int \mathbf{v}(\mathbf{v}\cdot\mathbf{v})f_\alpha(\mathbf{r},\mathbf{v},t)d^3\mathbf{v} \qquad (4.7)$$

4.1.5. Pressure Tensor

The pressure tensor for particles of species α at the point $\mathbf{r}$ in configuration space at time t is

$$\mathbf{P}_\alpha(\mathbf{r},t) = \bar{n}_\alpha m_\alpha \int (\mathbf{v}-\mathbf{V}_\alpha)(\mathbf{v}-\mathbf{V}_\alpha) f_\alpha(\mathbf{r},\mathbf{v},t)d^3\mathbf{v} \qquad (4.8)$$

For a sypherically symmetric velocity distribution this reduces to a diagonal pressure tensor

$$\mathbf{P}_\alpha = \begin{bmatrix} p_\alpha & 0 & 0 \\ 0 & p_\alpha & 0 \\ 0 & 0 & p_\alpha \end{bmatrix} \qquad (4.9)$$

and p_α is the scalar pressure given by

$$p_\alpha = \frac{m_\alpha \bar{n}_\alpha}{3} \int (\mathbf{v}-\mathbf{V}_\alpha)^2 f_\alpha d^3\mathbf{v} = n_\alpha \kappa T_\alpha \qquad (4.10)$$

The lack of spherical symmetry of the pressure tensor is often related to collision rates (e.g., to the viscosity of the fluid), and therefore the pressure tensor is normally broken up into two parts, one traceless, the other diagonal: $\mathbf{P}_\alpha = \mathbf{\Pi} + \mathbf{I}p_\alpha$, where p_α is defined by (4.10), and

$$\mathbf{\Pi} = \int \bar{n}_\alpha m_\alpha f_\alpha \left[(\mathbf{v}-\mathbf{V}_\alpha)(\mathbf{v}-\mathbf{V}_\alpha) - \frac{1}{3}\mathbf{I}(\mathbf{v}-\mathbf{V}_\alpha)\cdot(\mathbf{v}-\mathbf{V}_\alpha) \right]d^3\mathbf{v} \qquad (4.11)$$

where $\mathbf{\Pi}$ includes the off-diagonal terms of pressure tensor.

4.2.Macroscopic Equations for a Plasma: Fluid Equations

Just as the velocity moments of the distribution function give the macroscopic variables, so do the velocity moments of the plasma kinetic equation (i.e., Boltzmann equation) gives the equations that are satisfied by the macroscopic variables, and that describe the time evolution of the plasma from a macroscopic point of view. Because the equations obtained are identical with the continuum hydrodynamic equations, the theories using the macroscopic equation are called *fluid theories*.

4.2.1. Continuity Equation (0th Moment)

The integral of Boltzmann equation over all velocity space is

$$\int \left(\frac{\partial f_\alpha}{\partial t} + \mathbf{v} \cdot \frac{\partial}{\partial \mathbf{r}} f_\alpha + \frac{q_\alpha}{m_\alpha} \left\langle \mathbf{E} + \frac{\mathbf{v} \times \mathbf{B}}{c} \right\rangle \cdot \frac{\partial}{\partial \mathbf{v}} f_\alpha = \frac{\delta f_\alpha}{\delta t} \right) d^3 \mathbf{v} \qquad (4.12)$$

where $f_\alpha \equiv f_\alpha(\mathbf{r}, \mathbf{v}, t)$ is the distribution function and $\delta f_\alpha / \delta t$ represents the collisional terms. The right side of Equation (4.12) and the third term on the left-hand side of it both vanish, since both are of the form

$$\int \left[\frac{\partial}{\partial \mathbf{v}_1} \cdot \int a_1(\mathbf{r}_1, \cdots, \mathbf{r}_N) f d\mathbf{r}_2 \cdots d\mathbf{r}_N d^3 \mathbf{v}_2 \cdots d\mathbf{v}_N \right] d^3 \mathbf{v}_1 \qquad (4.13)$$

which is zero, since $f(\mathbf{v}_1 = \pm\infty) = 0$. This shows that collisions change the velocity of the particles in the system but do not directly affect the spatial density. Eq. (4.12) is nothing but the continuity equation obtained after integrating over $d^3 \mathbf{v}$, is

$$\frac{\partial}{\partial t} n_\alpha(\mathbf{r}, t) + \nabla \cdot n_\alpha(\mathbf{r}, t) \mathbf{V}_\alpha(\mathbf{r}, t) = 0 \qquad (4.14)$$

Note that $\nabla \equiv \partial/\partial x + \partial/\partial y + \partial/\partial z$ has been used in this macroscopic equation, along with the fact that

$$\int \mathbf{v} \cdot \frac{\partial}{\partial \mathbf{r}} f d^3 v = \frac{\partial}{\partial \mathbf{r}} \cdot \int f \mathbf{v} d^3 v = \nabla \cdot n\mathbf{V} \qquad (4.15)$$

This continuity equation represents conservation of particles. Source or sink terms on the right-hand side of Equation (4.15) would represent ionization or recombination. The equation for mass continuity is obtained from Equation (4.15) by multiplying through by the mass per particle m_α ; that is,

$$\frac{\partial}{\partial t}(\rho_{m\alpha}) + \nabla \cdot (\rho_{m\alpha} V_\alpha) = 0 \qquad (4.16)$$

where $\rho_{m\alpha} = n_\alpha m$ is the mass density. The equation for continuity of charge is obtained from Equation (4.15) by multiplying through by the charge per particle q_α ; that is,

$$\frac{\partial}{\partial t}(\rho_{q\alpha}) + \nabla \cdot (\rho_{q\alpha} V_\alpha) = 0 \qquad (4.17)$$

where $\rho_{q\alpha} = n_\alpha q_\alpha$ is the electric charge density.

4.2.2. Momentum Transfer Equation

The integral over all velocity space of the product of the plasma kinetic equation (Boltzmann equation) and the momentum $m_\alpha v$ of a particle of species α is

$$\int m_\alpha \mathbf{v} \left(\frac{\partial f_\alpha}{\partial t} + \mathbf{v} \cdot \frac{\partial}{\partial \mathbf{r}} f_\alpha + \frac{q_\alpha}{m_\alpha} \left\langle \mathbf{E} + \frac{\mathbf{v} \times \mathbf{B}}{c} \right\rangle \cdot \frac{\partial}{\partial \mathbf{v}} f_\alpha \right) d^3 v = \int m_\alpha \mathbf{v} \frac{\delta f_\alpha}{\delta t} d^3 v \ . \ (4.18)$$

With the aid of the continuity equation and in terms of previously defined variables, Equation (4.18) reduces to the momentum transfer equation for particles of species α ; that is,

$$n_\alpha m_\alpha \frac{\partial}{\partial t}(V_\alpha) + n_\alpha m_\alpha V_\alpha \cdot \nabla V_\alpha - n_\alpha q_\alpha \left\langle E + \frac{V_\alpha \times B}{c} \right\rangle + \nabla \cdot P_\alpha$$

$$= m_\alpha \int \overline{n}_\alpha v \frac{\partial f_\alpha}{\partial t} d^3 v \approx -\sum_\beta n_\alpha m_\alpha (V_\alpha - V_\beta) \langle v_{\alpha\beta} \rangle \tag{4.19}$$

where $\langle v_{\alpha\beta} \rangle$ is a mean collision frequency for momentum transfer from all other types of plasma particles. By conservation of momentum, the right-hand side of (4.19) vanishes for collisions between like particles and, for instance, represents a momentum loss for a fast-moving population due to collisions with a slower moving group of particles. The right-hand side of Equation (4.19) is often a valid simplification of this resistive term. In (4.19), P_α is the pressure tensor, and the average fields $\langle E \rangle$, $\langle B \rangle$ must be consistent with the average plasma properties n_α, V_α, etc., through Maxwell's equations,

$$\nabla \cdot \langle E \rangle = \sum_\alpha 4\pi n_\alpha q_\alpha + 4\pi \rho_{ext} \tag{4.20}$$

$$\nabla \times \langle B \rangle = \frac{1}{c} \frac{\partial \langle E \rangle}{\partial t} + \frac{4\pi}{c} \sum_\alpha n_\alpha q_\alpha V_\alpha + \frac{4\pi}{c} J_{ext} \tag{4.21}$$

The first two terms in Equation (4.19) combine to form a 'comoving' derivative (that is, $\partial/\partial t + V \cdot \partial/\partial r \equiv D/Dt$). The combined terms represent the change of momentum per unit time in the element moving with velocity V_α. The next term is the change of momentum per unit volume per unit time due to forces exerted by the average fields. The divergence of the pressure tensor gives the change of momentum per unit volume per unit time due to spatial inhomogeneities. This term includes the effect of viscosity. If particle collisions are sufficiently frequent, the pressure term reduces to the gradient of a scalar pressure (that is, $\nabla \cdot P \to \nabla p$). This is a frequently used approximation. In this thesis only simple closure schemes are used; even these lead to considerable complexity. It should be clear that the fluid theory, though of great practical use, relies heavily on the cunning of its user

It is clearly advantageous to choose as simple a closure scheme as possible. However, the choice of model determines the plasma properties that can be studied, since the approximations used eliminate certain features of plasma behavior.

Even without specifying a closure scheme, there are two general approaches to a macroscopic description of a plasma. In one, the ions and electrons are treated as separate but interacting fluids, each having its own set of equations and properties. In the other, the plasma is described as one fluid with a net density, velocity, and current at each point. In this thesis, the second approach is considered.

4.3. One-Fluid Plasma Theory:

4.3.1. Magnetohydrodynamics

By combining the density and velocity of ions and electrons, fluid equations whose variables are the total mass density, center-of-mass velocity, electric current, and charge density can be obtained. The one-fluid theory so obtained is a simpler starting point for many problems, and will be examined in detail.

4.3.2. One-fluid Variables

The mass density in the fluid is defined by

$$\rho_m(\mathbf{r},t) = \sum_\alpha n_\alpha m_\alpha = n_e m_e + n_i m_i \qquad (4.22)$$

where the subscripts e and i refer to electrons and ions respectively. The charge density is

$$\rho_q(\mathbf{r},t) = \sum_\alpha n_\alpha q_\alpha = e(n_i - n_e) \qquad (4.23)$$

The center-of-mass velocity is given by

$$V(r,t) = \frac{\sum_\alpha n_\alpha m_\alpha V_\alpha}{\sum_\alpha n_\alpha m_\alpha} = \frac{n_e m_e V_e + n_i m_i V_i}{n_e m_e + n_i m_i} \tag{4.24}$$

Note that this form of velocity is identical to Equation (4.5) with the only exception that the sum is used instead of integration. The total current is

$$J = \sum q_\alpha n_\alpha V_\alpha \tag{4.25}$$

and the pressure of electrons and ions in the center-of-mass frame is

$$P_\alpha^{CM} = \bar{n}_\alpha m_\alpha \int (v - V)(v - V) f_\alpha dv \tag{4.26}$$

and the total pressure is

$$P = \sum_\alpha P_\alpha^{CM} \tag{4.27}$$

Note that Equation (4.26) is identical to Equation (4.8).

4.3.3. One-Fluid Equations

The differential equations satisfied by the one-fluid variables are obtained by adding and subtracting the fluid Equations (4.1) to (4.5), which separately describe the behavior of ions and electrons. Equations for continuity of mass and charge density are simply obtained from (4.16). Multiplying (4.16) by m_α and adding the equations for ions and electrons gives

$$\frac{\partial \rho_m}{\partial t} + \nabla \cdot \rho_m V = 0 \tag{4.28}$$

while multiplying (4.1) by q_α and adding the equations for ions and electrons gives

$$\frac{\partial}{\partial t} \rho_q + \nabla \cdot J = 0 \tag{4.29}$$

Similarly, summing Equation (4.19) over ions and electrons gives the equation for momentum transport in the one-fluid theory.

$$\rho_m \frac{\partial}{\partial t} \mathbf{V} + \rho_m (\mathbf{V} \cdot \nabla)\mathbf{V} = \rho_q \mathbf{E} + \frac{\mathbf{J} \times \mathbf{B}}{c} - \nabla \cdot \mathbf{P} \qquad (4.30)$$

The current density is obtained from the *generalized Ohm's law* for a plasma, since it relates the current to the electric field. The collision term, which is $\delta \mathbf{J}/\delta t \big|_{collisions}$, is often estimated by a linear approximation

$$\sum_\alpha \bar{n}_\alpha q_\alpha \int \mathbf{v} \frac{\partial f_\alpha}{\partial t} \bigg|_c d^3\mathbf{v} \approx -\upsilon \mathbf{J} \qquad (4.31)$$

where υ is an average collision frequency. In terms of υ, the resistivity and conductivity are defined by

$$\eta = \frac{\upsilon m_e}{ne^2}, \quad \sigma = \frac{1}{\eta} \qquad (4.32)$$

Note that the current density satisfies the Ohm's law, $\mathbf{E} = \eta \mathbf{J}$ in the, static, uniform-pressure limit. Equations (4.28) to (4.29) constitute a set of equations for the one-fluid variables, but of course these equations are also not *closed*; i.e.,there are more unknowns than equations. This situation is not remedied by taking higher moments of the kinetic equations (4.12), since each new equation contains an additional variable. Closure of (4.28) to (4.29) is generally achieved by assuming an equation of state. Sometimes the choice of equation of state (EOS) is plausible. In any event, the choice has a strong effect on the results found from the fluid equations, and should not be made arbitrarily. Thermodynamics is an effective tool in deriving physically meaningful EOS.

4.4. Approximations Commonly Used In One-fluid Theory

Even with a choice of an equation of state, the fluid equations are cumbersome. In practice, these equations are simplified by a set of assumptions valid for a wide range of phenomena. Since the assumptions do limit the applicability of the equations, it is important to take note of them before writing down the commonly used form of the fluid equations:

$$\text{Quasineutrality,}\ \rho_{qe} = \rho_{qi} \tag{4.33}$$

A major simplification is achieved by assuming that the charge density vanishes, $\rho_q = 0$. However, since the charge density does not in fact vanish, the assumption that $n_e = Zn_i$ represents an approximation and a loss of information. Yet, because the plasma as a whole is neutral $\left(N_e = ZN_i\right)$, there must be some scale on which (4.33) is valid. This scale is the Debye length: an excess charge at rest is shielded, i.e., surrounded by a charge equal and opposite its own, in a distance λ_D. Thus, if slow motions of fluid elements of size greater than λ_D are studied, it may be assumed that $n_e = n_i$.

$$\frac{n_e - n_i}{n_e} \ll 1 \ \text{if}\ \frac{\omega_p^2}{\kappa T / m}L^2 \gg 1 \tag{4.34}$$

where L is the length scale under study. If a system is being studied with a spatial resolution better than λ_D, or if a phenomenon involves spatial variations on scales $L \sim \lambda_D$, then quasineutrality is a bad assumption. Note that, in general, the assumption (4.33) implies also

$$\nabla \cdot \mathbf{J} = 0 \tag{4.35}$$

another approximation frequently made is

$$n e \mathbf{V} \cdot \nabla \mathbf{V} = 0 \ \text{or} \qquad \nabla \cdot \left(\mathbf{JV}\right) = 0 \tag{4.36}$$

these simplifications are valid for a wide class of phenomena. For example, in problems involving perturbations about an initial state, the initial state will have **V**=0 in some frame, and in that frame terms $\mathbf{V} \cdot \mathbf{V}$ are *second-order* in the perturbation.

A trivial approximation is to neglect m_e / m_i, since

$$\frac{m_e}{m_i} << 1 \tag{4.37}$$

However, when used in connection with (4.33), this implies further that

$$\rho_m = n_i m_i \tag{4.38}$$

In many examples, only phenomena of very low frequency ω and very long spatial scale L are considered. In these cases, since $\mathbf{J} = (c / 4\pi)(\nabla \times \mathbf{B})$ from Maxwell's equations, both $\mathbf{J} \times \mathbf{B}$ and $d\mathbf{J} / dt$ are neglected in Ohm's law:

$$\frac{1}{|\mathbf{J}|}\frac{1}{\omega_p}\frac{d\mathbf{J}}{dt} \approx \frac{\omega}{\omega_p} << 1 \qquad \frac{\mathbf{J} \times \mathbf{B}}{c} \approx \frac{B^2}{L} << ne\frac{\mathbf{V} \times \mathbf{B}}{c} \tag{4.39}$$

Of course, there are problems in which pressure gradients dominate electric fields, and the $\mathbf{J} \times \mathbf{B}$ term will be important. Another frequent assumption is of isotropic pressure,

$$\mathbf{V} \cdot \mathbf{P}_\alpha = \nabla p_\alpha \tag{4.40}$$

this approximation neglects viscosity effects; it is certainly valid when interparticle collisions are sufficiently frequent. This statement cannot be made quantitative without some theory for collisional effects. If the frequency of ion-ion collisions is greater than the cyclotron frequency or any other frequency considered in the problem, one particular model, the Navier-Stokes (NS) theory, gives

$$R_e \equiv LV_0 \frac{m_i}{\kappa T} v_{ii} \gg 1 \qquad (4.41)$$

as the criterion for neglecting off-diagonal terms in the pressure tensor. R is called the Reynolds number. In (4.41) L is a characteristic length, and V_0 is a characteristic velocity of the medium under examination. Because of the simplifications it produces, the approximation (4.40) is used in the study of nearly collision-free plasma, where (4.41) is not satisfied. It is a fortunate fact that the plasma equations with $\nabla \cdot P = \nabla p$ agree with a wide range of experiments, despite the lack of a clear basis for that approximation. It is presumed that the plasma frequency ω_p acts as a 'collision frequency' in wiping out off-diagonal pressure tensor elements.

When the terms $J \times B$, $\partial J / \partial t$, and ∇p are all neglected, the simplified form of Ohm's law,

$$J = \sigma \left(E + \frac{V \times B}{c} \right) \qquad (4.42)$$

is obtained, with σ defined by (4.32). Even this simple form of Ohm's law leads to some interesting conclusions about the dynamics of a plasma in a strong magnetic field. In discussing the validity of the simplified Ohm's law, it should be noted that dimensional analysis alone shows that the $J \times B$ term can be neglected when the characteristic length scale within which the field properties change is sufficiently long. The criterion for (4.42) can be expressed explicitly in terms of the length and velocity scales of interest for the problem. Let L be the length scale for spatial variation of the plasma parameters and V_0 be a characteristic velocity of the plasma fluid. Ohm's law would be made simpler if the conductivity were infinite. This approximation is valid as follows:

$$\frac{4\pi J}{\sigma} \text{ can be neglected in Ohm's law when } R_M \equiv \frac{4\pi \sigma L V_0}{c^2} \gg 1 \qquad (4.43)$$

R_M is called the magnetic Reynolds number, and if $R_M \gg 1$, Ohm's law is

$$E + \frac{V \times B}{c} = 0 .$$

(4.44)

4.5. Simplified One-Fluid Equations And The MHD Equation

A simplified set of one-fluid equations can be obtained in order to describe plasma phenomena on a long space scale $(L \to \infty)$. From the discussion in the preceding section, the approximation $n_e = n_i$ is valid on a long space scale. In addition, gradient terms (for example, $\nabla p, \nabla B, \nabla \cdot V$, etc.) can be treated as small compared with field terms (for example, B, E, J, V, etc.). With these approximations, and the neglect of the ratio m_e / m_i compared with unity, the one-fluid equations become

$$\frac{\partial \rho_m}{\partial t} + \nabla \cdot \rho_m V = 0$$

(4.45)

$$\rho_m \frac{DV}{Dt} = \frac{J \times B}{c} - \nabla(p_i + p_e) - [\nabla \cdot P_i + \nabla \cdot P_e - \nabla(p_i + p_e)]$$

(4.46)

$$E + \frac{V \times B}{c} = \eta J + \frac{m_e}{ne^2} \frac{DJ}{Dt}$$

(4.47)

$$\nabla \times B = \frac{1}{c} \frac{\partial E}{\partial t} + \frac{4\pi J}{c}$$

(4.48)

$$\nabla \times E = -\frac{1}{c} \frac{\partial B}{\partial t}$$

(4.49)

along with the boundary condition

$$\nabla \cdot B = 0$$

(4.50)

and the definition of the comoving derivative

$$\frac{D}{Dt} \equiv \frac{\partial}{\partial t} + \mathbf{V} \cdot \nabla \tag{4.51}$$

It is not inconsistent to neglect ∇p compared with $\mathbf{V} \times \mathbf{B}$ in Ohm's law (4.47) and still retain it in the momentum transport Equation (4.46). This is because all terms on the right-hand side of (4.46) are proportional to gradients of the physical variable (since $4\pi \mathbf{J}/c \approx \nabla \times \mathbf{B}$). Equation (4.47), on the other hand, includes terms not proportional to gradients. These terms are treated as *large*, and gradients are neglected compared with them.

The set of Equations (4.45) to (4.50) are closed by an equation of state or by some other model relating the pressure to the density. The usual approximation of magnetohydrodynamics is to use the assumption of incompressible fluid

$$\nabla \cdot \mathbf{V} = 0 \tag{4.52}$$

or adiabatic fluid

$$\frac{d}{dt} p \rho_m^{-\gamma} = 0 \tag{4.53}$$

or isothermal fluid

$$\frac{d}{dt} \frac{p}{\rho_m} = 0 \tag{4.54}$$

or some other closure equation. The one-fluid equation obtained from the transport theory can also be derived from the continuum approach by assuming control volumes in the fluid and considering possible forces on them. This procedure will be explained in detail in the fifth unit.

5. BASIC CONSERVATION LAWS

The purpose of this chapter is to derive the set of equations which results from the physical laws of conservation of mass, momentum, and energy. In order to realize this objective, it is necessary to discuss certain preliminary topics. The first topic of discussion is the two basic ways in which the conservation equations may be derived, the statistical method and the continuum method. Having established the basic method to be employed and the tools to be used, the basic conservation laws are then derived. The conservation of mass yields the so-called continuity equation. The conservation of momentum leads ultimately to the Navier-Stokes equations, while the conservation of thermal energy leads to the energy equation. The derivation is followed by a discussion of charged particle rotations and Maxwell's equations to be added to the conservation equations, and finally a summary of the basic conservation laws that can be used for charged or neutral fluid flows is given.

5.1.   Statistical and Continuum Method

There are basically two ways of deriving the conservation equations which govern the motion of a fluid. One of these methods approaches the question from the molecular point of view. That is, this method treats the fluid as consisting of molecules whose motion is governed by the laws of dynamics. The macroscopic phenomena are assumed to arise from the molecular motion of the molecules, and the theory attempts to predict the macroscopic behavior of the fluid from the laws of mechanics and probability theory.

For a fluid which is in a state not too far removed from equilibrium, this approach yields the equations of mass, momentum, and energy conservation. The molecular approach also yields expressions for the transport coefficients, such as the coefficient of viscosity and the thermal conductivity, in terms of molecular quantities such as the forces acting between molecules or molecular diameters. The theory is well developed for light gases, but it is incomplete for polyatomic gas molecules and for liquids. It must be noted that this theory was explained in detail in unit four.

The alternative method which is used to derive the equations which govern the motion of a fluid uses the continuum concept. In the continuum approach, individual molecules are ignored and it is assumed that the fluid consists of continuous matter. At each point of this continuous fluid there is supposed to be a unique value of the velocity, pressure, density, and other so-called 'field variables.' The continuous matter is then required to obey the conservation laws of mass, momentum, and energy, which give rise to a set of differential equations governing the field variables. The solution to these differential equations then defines the variation of each field variable with space and time which corresponds to the mean value of the molecular magnitude of that field variable at each corresponding position and time.

The molecular statistical method is rather elegant, and it may be used to treat gas flows in situations where the continuum concept is no longer valid. However, as was mentioned before, the theory is incomplete for dense gases and for liquids. The continuum approach requires that the mean free path of the molecules be very small compared with the smallest physical-length scale of the flow field (such as the diameter of a cylinder or other body about which the fluid is flowing.) Only in this way can meaningful averages over the molecules at a 'point' be made and the molecular structure of the fluid be ignored. However, if this condition is satisfied, there is no distinction amongst light gases, dense gases, or even liquids the results apply equally to all. Since the vast majority of phenomena encountered in fluid mechanics fall within the continuum domain and may involve liquids as well as gases, the continuum method will be used in this thesis. With this background, the meaning and validity of the continuum concept will be explored in some detail.

The field variables such as the density ρ and the velocity vector $\mathbf{v}$ will in general be functions of the spatial coordinates and time. In symbolic form this is written as $\rho = \rho(\mathbf{r}, t)$ and $\mathbf{v} = \mathbf{v}(\mathbf{r}, t)$, where $\mathbf{r}$ is the position vector whose cartesian coordinates are x, y, and z. At any particular point in space these continuum variables are defined in terms of the properties of the various molecules which occupy a small volume in the neighbourhood of that point.

Consider a small volume of fluid $\Delta\Omega$ containing a large number of molecules. Let Δm and $\mathbf{v}$ be the mass and velocity of any individual molecule contained within the volume $\Delta\Omega$ as indicated in Figure 5.1. The density and the velocity at a point in the continuum are then defined by the following limits:
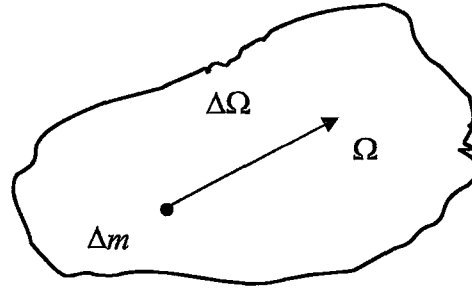
Figure.5.1. An individual molecule in a small volume $\Delta\Omega$ having a mass Δm and a velocity $\mathbf{v}$.

$$\rho = \lim_{\nabla\Omega \to \Omega_0}\left(\frac{\sum \Delta m}{\Delta\Omega}\right) \qquad \mathbf{v} = \lim_{\nabla\Omega \to \Omega_0}\left(\frac{\sum \mathbf{v}\Delta m}{\sum \Delta m}\right) \qquad (5.1)$$

where Ω_0 is a volume which is sufficiently small that $\Omega_0^{1/3}$ is small compared with the smallest significant length scale in the flow field but is sufficiently large that it contains a large number of molecules. The summations in the above expressions are taken over all the molecules contained within the volume $\Delta\Omega$. The other field variables may be defined in terms of the molecular properties in an analogous way. A sufficient condition for the continuum approach to be valid is;

$$\frac{1}{N} \ll \Omega_0 \ll L^3 \qquad (5.2)$$

where N is the number of molecules per unit volume and L is the smallest significant length scale in the flow field, which is usually called the *macroscopic length scale*. The characteristic *microscopic length scale* is the mean free path between collisions of the molecules. Then the above condition states that the continuum concept will certainly be valid if some volume Ω_0 can be found which is much larger than the volume occupied by a single molecule of the fluid but which is much smaller than the cube of the smallest

macroscopic length scale (such as cylinder diameter). Since a cube of gas, at normal temperature and pressure, whose side is 2 micrometers contains about 2×10^8 molecules and the corresponding Figure for a liquid is about 2×10^{11} molecules, the continuum condition is readily met in the vast majority of flow situations encountered in physics and engineering. It may be expected to break down in situations where the smallest macroscopic length scale approaches microscopic dimensions, such as in the structure of a shock wave, and where the microscopic length scale approaches macroscopic dimensions, such as when a rocket passes through the edge of the atmosphere. In this thesis, the incompressible magnetized and neutral flows are considered and the flows do not exhibit steep gradients.

5.2. Eulerian and Lagrangian Coordinates

Having selected the continuum approach as the method which will be used to derive the basic conservation laws, one is next faced with a choice of reference frames in which to formulate the conservation laws. There are two basic coordinate systems which may be employed, these being Eulerian and Lagrangian coordinates.

In the Eulerian framework the independent variables are the spatial coordinates x, y, z, and time t. This is the familiar framework in which most problems are solved. In order to derive the basic conservation equations in this framework, attention is focused on the fluid which passes through a control volume which is fixed in in space. The fluid inside the control volume at any instant in time will consist of different fluid particles from that which was there at some previous instant in time. If the principles of conservation of mass, momentum, and energy are applied to the fluid which passes through the control volume, the basic conservation equations are obtained in Eulerian coordinates in order to determine the dynamics of the fluid.

In the Lagrangian approach, attention is fixed on a particular mass of fluid as it flows. Suppose we could color a small portion of the fluid without changing its density. Then in the Lagrangian framework we follow this colored portion as it flows and changes its shape, but we are always considering the same particles of fluid. The principles of

mass, momentum, and energy conservation are then applied to this particular element of fluid as it flows, resulting in a set of conservation equations in Lagrangian coordinates. In this reference frame x, y, z, and t are no longer independent variables, since if it is known that our colored portion of fluid passed through the coordinates x_0, y_0, and z_0 at some time t_0, then its position at some later time may be calculated if the velocity components u, v, and w are known.

The choice of which coordinate system to employ is largely a matter of taste. It is probably more convincing to apply the conservation laws to a control volume which always consists of the same fluid particles rather than one through which different fluid particles pass. This is particularly true when invoking the law of conservation of energy, which consists of applying the first law of thermodynamics, since the same fluid particles are more readily justified as a thermodynamic system. For this reason, the Lagrangian coordinate system will be used to derive the basic conservation equations. Although the Lagrangian system will be used to derive the basic equations, the Eulerian system is the one which is used in this thesis for solving the majority of problems.

5.3. Control Volumes

The concept of a control volume, as required to derive the basic conservation equations, has been mentioned in connection with both the Lagrangian and the Eulerian approaches. Irrespective of which coordinate system is used, there are two principal control volumes from which to choose. One of these is a parallelpiped of sides $\delta x, \delta y$, and δz. Each fluid property, such as the velocity or pressure, is expanded in a Taylor series about the center of the control volume to give expressions for that property at each face of the control volume. The conservation principle is then invoked, and when $\delta x, \delta y$, and δz are permitted to become vanishingly small (i.e., the volume $\rightarrow 0$), the differential equation for that conservation principle is obtained. Frequently, shortcuts are taken and the control volume is taken to have sides of length dx, dy, and dz with only the first term of the Taylor series being carried out.

The second type of control volume is arbitrary in shape, and each conservation principle is applied to an integral over the control volume. For example, the mass within the control volume is $\int_\Omega \rho d\Omega$, where ρ is the fluid density and the integration is carried out over the entire volume Ω of the fluid contained within the control volume. The result of applying each conservation principle will be an integro-differential equation of the type

$$\int_\Omega \Re \alpha d\Omega = 0 \tag{5.3}$$

where $\Re$ is some differential operator and α is some property of the fluid. But since the control volume $d\Omega$ was arbitrarily chosen, the only way this equation can be satisfied is by setting $\Re\alpha = 0$, which gives the differential equation of the conservation law. If the integrand in the above equation was not equal to zero, it would be possible to redefine the control volume Ω in such a way that the integral of $\Re\alpha$ was equal to zero. In this thesis, the arbitrary control volume will be used in the derivation of the basic conservation laws.

5.4. Conservation of Mass

Consider a specific mass of fluid whose volume Ω is arbitrarily chosen. If this given fluid mass is followed as it flows, its size and shape will be observed to change but its mass will remain unchanged. This is the principle of mass conservation which applies to fluids in which no nuclear reactions are taking place. The mathematical equivalence of the statement of mass conservation is to set the Lagrangian derivative D/Dt of the mass of fluid contained in Ω, which is $\int_\Omega \rho d\Omega$, equal to zero. That is, the equation which expresses conservation of mass is

$$\frac{D}{Dt}\left[\int_\Omega \rho d\Omega\right] = 0 \quad \text{where} \quad \frac{D\alpha}{Dt} \equiv \frac{\partial \alpha}{\partial t} + \mathbf{V}.\nabla\alpha \tag{5.4}$$

is the Lagrangian derivative of the scalar quantity, α. This equation may be converted to a volume integral in which the integrand contains only Eulerian derivatives by use of Reynolds' transport theorem in which the fluid property α is, in this case, the mass density ρ.

$$\int_\Omega \left[\frac{\partial \rho}{\partial t} + \frac{\partial}{\partial r_k} (\rho v_k) \right] d\Omega = 0 \qquad (5.5)$$

Since the volume Ω is arbitrarily chosen, the only way in which the above equation can be satisfied for all possible choices of Ω is for the integrand to be zero. Then the equation expressing conservation of mass becomes

$$\frac{\partial \rho}{\partial t} + \frac{\partial}{\partial r_k} (\rho v_k) = \frac{\partial \rho}{\partial t} + \nabla \cdot (\rho V) = 0. \qquad (5.6)$$

This equation expresses more than the fact that mass is conserved. Since it is a partial differential equation, the implication is that the velocity is continuous. For this reason the above equation is usually called the *continuity equation*. The derivation which has been given here is for a single-phase fluid in which no change of phase is taking place. If two phases were present, such as water and steam, the starting statement would be that the rate at which the mass of fluid 1 is increasing is equal to the rate at which the mass of fluid 2 is decreasing. The generalization to cases of multiphase fluids and to cases of nuclear reactions is obvious. Since such cases cause no changes in the basic ideas or principles, they will not be included in this treatment of the fundamentals.

In many practical cases of fluid flow, the variation of density of the fluid may be ignored, as for most cases of the flow of liquids. In such cases the fluid is said to be *incompressible,* which means that as a given mass of fluid is followed, not only will its mass be observed to remain constant but its volume, and hence its density, will be observed to remain constant. Mathematically, this statement may be written as

$$\frac{D\rho}{Dt} = 0. \qquad (5.7)$$

In order to use this special simplification, the continuity equation is first expanded by use of a vector identity which is given;

$$\frac{\partial \rho}{\partial t} + v_k V \cdot \nabla \rho + \rho \nabla \cdot V = 0 .$$

(5.8)

The first and second terms in this form of the continuity equation will be recognized as being the Eulerian form of the material derivative as given by Equation (5.4). That is, an alternative form of Equation (5.8) is

$$\frac{D\rho}{Dt} + \rho \nabla \cdot V = 0 .$$

(5.9)

This mixed form of the continuity equation in which one term is given as a Lagrangian derivative and the other as an Eulerian derivative is not useful for actually solving fluid-flow problems. However, it is frequently used in the manipulations which reduce the governing equations to alternative forms, and for this reason it has been identified for future reference. Since $D\rho / Dt = 0$ for incompressible fluids, Equation (5.9) above shows that the continuity equation assumes the simplier form $\rho \nabla \cdot V = 0$. Since ρ cannot be zero in general, the continuity equation for an incompressible fluid becomes

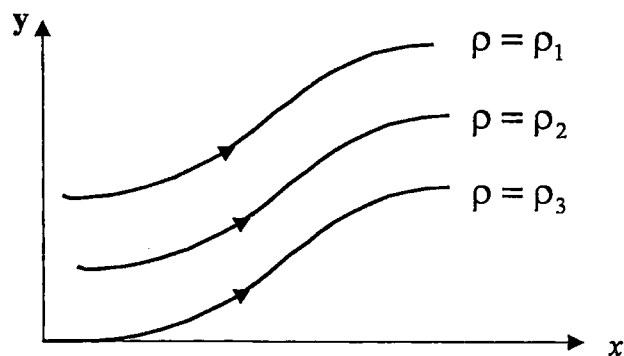$$\nabla \cdot V = 0 \quad (\text{incompressible})$$

(5.10)

Figure.5.2. The constant density streamlines.

It should be noted that equation above is valid not only for the special case of $D\rho/Dt = 0$ in which ρ =constant everywhere, but also for stratified-fluid flows of the type depicted in Figure.5.2. A fluid particle which follows the lines $\rho = \rho_1$ or $\rho = \rho_2$ will have its density remain fixed at $\rho = \rho_1$ or $\rho = \rho_2$ so that $D\rho/Dt = 0$. However, ρ is not constant everywhere, so that $\partial\rho/\partial x \neq 0$ and $\partial\rho/\partial y \neq 0$. Such density stratifications may occur in the ocean (owing to salinity variations) or in the atmosphere (owing to temperature variations). However, in the majority of cases in which the fluid may be considered to be incompressible, the density is constant everywhere. Equation (5.4), in either the general form (5.6) or the incompressible form (5.10), is the first condition which has to be satisfied by the velocity and the density. No dynamical relations have been used to this point, but the conservation-of-momentum principle will utilize dynamics.

5.5. Conservation of Momentum

The principle of conservation of momentum is, in effect, an application of Newton's second law of motion to an element of the fluid. That is, when considering a given mass of fluid in a Lagrangian frame of reference, it is stated that the rate at which the momentum of the fluid mass is changing is equal to the net external force acting on the mass. Some individuals prefer to think of forces only and restate this law in the form that the inertia force (due to acceleration of the element) is equal to the net external force acting on the element.

The external forces which may act on a mass of the fluid may be classed as either body forces, such as gravitational or electromagnetic forces, or surface forces, such as pressure forces or viscous stresses. Then if $\mathbf{F}$ is a vector which represents the resultant of the body forces per unit mass, the net external body force acting on a mass of volume Ω will be $\int_\Omega \rho \mathbf{F} d\Omega$. Also, if $\mathbf{P}$ is a surface vector which represents the resultant surface force per unit area, the net external surface force acting on the surface S containing Ω will be $\int_S \mathbf{P} ds$. According to the statement of the physical law which is being imposed in this section, the sum of the resultant forces evaluated above is equal to the rate of change of

momentum (or inertia force). The mass per unit volume is ρ and its momentum is ρv, so that the momentum contained in the volume Ω is $\int_\Omega \rho v d\Omega$. Then, if the mass of the arbitrarily chosen volume Ω is observed in the Lagrangian frame of reference, the rate of change of momentum of the mass contained within Ω will be $\left(D/Dt \int_\Omega \rho v d\Omega \right)$. Thus the mathematical equation which results from imposing the physical law of conservation of momentum is

$$\frac{D}{Dt} \int_\Omega \rho v d\Omega = \int_s \mathbf{P} ds + \int_\Omega \rho \mathbf{F} d\Omega \qquad (5.11)$$

5.5.1. Stress and Pressure

In order to determine the correct behavior of fluid, the pressure and stress effects of the medium in which it moves must be considered. In general, there are nine of stress σ at any given point, one normal component and two shear components on each coordinate plane. These nine components of stress are easily illustrated by assuming that the fluid element considered is made of a cubical element in which the faces of the cube are orthogonal to the cartesian coordinates, as shown in Figure.5.3, and in which the stress components will act at a point as the length of the fluid cube tends to zero. Note that the normal components of stress, $\sigma_{11}, \sigma_{22}, \sigma_{33}$ are nothing but scalar pressure defined in Equation (4.9) and (4.10). In Figure 5.3 the cartesian coordinates x, y, and z have been denoted by $x_1, x_2,$ and x_3, respectively. This permits the components of stress to be identified by a double-subscript notation. In this notation, a particular component of the stress may be represented by the quantity σ_{ij}, in which the first subscript indicates that this stress component acts on the plane $x_i = $ constant and second subscript indicates that it acts in the x_j direction. The fact that the stress may be represented by the quantity σ_{ij}, in which i and j may be 1,2, or 3, means that the stress at a point may be represented by a tensor of rank 2. However, on the surface of our control volume it was observed that there would be a vector force at each point, and this force was represented by $\mathbf{P}$. The surface

force vector **P** may be related to the stress tensor σ_{ij} as follows: The three stress components acting on the plane $x_1 =$ constant are σ_{11}, σ_{12}, and σ_{13}. Since the unit normal vector acting on this surface is n_1, the resulting force acting in the x_1 direction is $P_1 = \sigma_{11} n_1$. Likewise, the forces acting in the x_2, x_3 directions are, respectively,
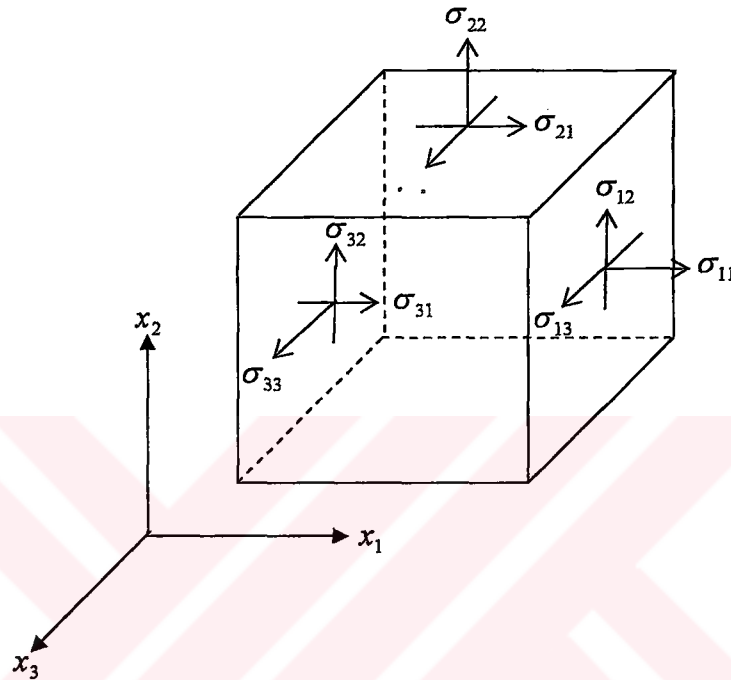
Figure.5.3. Representation of the nine components of stress which may act at on the surface of control volume of a fluid. $\sigma_{11}, \sigma_{22}, \sigma_{33}$ are scalar pressures.

$P_2 = \sigma_{12} n_1$ and $P_3 = \sigma_{13} n_1$. Then, for an arbitrarily oriented surface whose unit normal has components n_1, n_2, and n_3, the surface force will be given by $P_j = \sigma_{ij} n_i$ in which i is summed from 1 to 3. That is, in tensor notation the equation expressing conservation of momentum becomes

$$\frac{D}{Dt} \int_\Omega \rho v_j d\Omega = \int_S \sigma_{ij} n_i dS + \int_\Omega \rho f_i d\Omega \qquad (5.12)$$

The left-hand side of this equation may be converted to a volume integral in which the integrand contains only eulerian derivatives by use of Reynolds'transport theorem,

Equation (5.2), in which the fluid property α here is the momentum per unit volume ρv_j in the r_j direction. At the same time the surface integral on the right-hand side may be converted into a volume integral by use of Gauss' theorem.

In this way the equation which evolved from Newton's second law becomes

$$\int_\Omega \left[\frac{\partial}{\partial t}(\rho v_j) + \frac{\partial}{\partial r_k}(\rho v_j v_k) \right] d\Omega = \int_\Omega \frac{\partial \sigma_{ij}}{\partial r_i} d\Omega + \int_\Omega \rho f_i d\Omega \qquad (5.13)$$

All these volume integrals may be collected to express this equation in the form $\int_\Omega \left[\int_\Omega \frac{\partial \sigma_{ij}}{\partial r_i} + \int_\Omega \rho f_i \right] d\Omega = 0$, where the integrand is a differential equation in eulerian coordinates. As before, the arbitrariness of the choice of the control volume Ω is now used to show that the integrand of the above integro-differential equation must be zero. This gives the following differential equation to be satisfied by the field variables in order that the basic law of dynamics may be satisfied:

$$\frac{\partial}{\partial t}(\rho v_j) + \frac{\partial}{\partial r_k}(\rho v_j v_k) = \frac{\partial \sigma_{ij}}{\partial r_i} + \rho f_i \qquad (5.14)$$

The left-hand side of this equation may be further simplified if the two terms involved are expanded in which the quantity $\rho v_j v_k$ is considered to be the product of ρv_k and v_j.

$$\rho \frac{\partial v_j}{\partial t} + v_j \frac{\partial \rho}{\partial t} + v_j \frac{\partial}{\partial r_k}(\rho v_k) + \rho v_k \frac{\partial v_j}{\partial r_k} = \frac{\partial \sigma_{ij}}{\partial r_i} + \rho f_j \qquad (5.15)$$

The second and third terms on the left-hand side of this equation are now seen to sum to zero, since they amount to the continuity Equation (5.6) multiplied by the velocity v_j.

With this simplification, the equation which expresses conservation of momentum becomes

$$\rho\frac{\partial v_j}{\partial t} + \rho v_k \frac{\partial v_j}{\partial r_k} = \frac{\partial \sigma_{ij}}{\partial r_i} + \rho f_j \qquad (5.16)$$

It is useful to recall this equation came from an application of Newton's second law to an element of the fluid. The left-hand side of Equation (5.16) represents the rate of change of momentum of a unit volume of the fluid (or the inertia force per unit volume). The first term is the familiar temporal acceleration term, while the second term is a convective acceleration and accounts for local accelerations (around obstacles, etc.) even when the flow is steady. Note also that this second term is non-linear, since the velocity appears quadratically. On the right-hand side of Equation.(5.16) are the forces which are causing the acceleration. The first of these is due to the gradient of surface shear stresses while the second is due to body forces, such as gravity, which act on the mass of the fluid. A clear understanding of the physical significance of each of the terms in Equation (5.16) is essential when approximations to the full governing equations must be made. The surface-stress tensor σ_{ij} has not been fully explained up to this point, but it will be investigated in detail in a later section.

5.6 Conservation of Energy

The principle of conservation of energy is an application of the first law of thermodynamics to a fluid element as it flows. The first law of thermodynamics applies to a thermodynamic system which is originally at rest and, after some event, is finally at rest again. Under these conditions it is stated that the change in internal energy, due to the event, is equal to the sum of the total work done on the system during the course of the event and any heat which was added. Although a specified mass of fluid in a Lagrangian frame of reference may be considered to be a thermodynamic system, it is, in general, never at rest and therefore never in equilibrium. However, in the thermodynamic sense a flowing fluid is seldom far from a state of equilibrium, and the apparent difficulty may be

overcome by considering the instantaneous energy of the fluid to consist of two parts, intrinsic or internal energy and kinetic energy. That is, when applying the first law of thermodynamics, the energy referred to is considered to be the sum of the internal energy per unit mass ε and the kinetic energy per unit mass $\frac{1}{2}\mathbf{v} \cdot \mathbf{v}$. In this way the modified form of the first law of thermodynamics which will be applied to an element of the fluid states that the rate of change of the total energy (internal plus kinetic) of the fluid as it flows is equal to the sum of the rate at which work is being done on the fluid by external forces and the rate at which heat is being added by conduction.

With this basic law in mind, we again consider any arbitrary mass of fluid of volume Ω and follow it in a Lagrangian frame of reference as it flows. The total energy of this mass per unit volume is $\rho\varepsilon + \frac{1}{2}\rho\mathbf{v} \cdot \mathbf{v}$, so that the total energy contained in Ω will be

$$\int_{\Omega}\left(\rho\varepsilon + \frac{1}{2}\rho\mathbf{v} \cdot \mathbf{v}\right)d\Omega . \tag{5.17}$$

As was established in the previous section, there are two types of external forces which may act on the fluid mass under consideration. The work done on the fluid by these forces is given by the product of the velocity and the component of each force which is collinear with the velocity. That is, the work done is the scalar product of the velocity vector and the force vector. One type of force which may act on the fluid is a surface stress whose magnitude per unit area is represented by the vector $\mathbf{P}$. Then the total work done owing to such forces will be $\int_{S}\mathbf{v} \cdot \mathbf{P}dS$, where S is the surface area enclosing Ω. The other type of force which may act on the fluid is a body force whose magnitude per unit mass is denoted by the vector $\mathbf{F}$. Then the total work done on the fluid due to such forces will be $\int_{\Omega}\mathbf{v} \cdot \rho\mathbf{F}d\Omega$. Finally, an expression for the heat added to the fluid is required. Let the vector $\mathbf{q}$ denote the conductive heat flux *leaving* the control volume. Then the quantity of heat leaving the fluid mass per unit time per unit surface area will be $\mathbf{q} \cdot \hat{\mathbf{n}}$,

where $\hat{n}$ is the unit outward normal, so that the net amount of heat leaving the fluid per unit time will be $\int_S \mathbf{q} \cdot \hat{n} dS$.

Having evaluated each of the terms which appear in the physical law which is to be imposed, the statement may now be written down in analytic form. In doing so, it must be born in mind that the physical law is being applied to a specific, though arbitrarily chosen, mass of fluid so that Lagrangian derivatives must be employed. In this way the expression of the statement that the rate of change of total energy is equal to the rate at which work is being done plus the rate at which heat is being *added* becomes:

$$\frac{D}{Dt} \int_\Omega \left(\rho\varepsilon + \frac{1}{2}\rho \mathbf{v} \cdot \mathbf{v} \right) d\Omega = \int_S \mathbf{v} \cdot \mathbf{P} dS + \int_\Omega \mathbf{v} \cdot \rho \mathbf{F} d\Omega - \int_S \mathbf{q} \cdot \hat{n} dS \quad (5.18)$$

This equation may be converted to one involving Eulerian derivatives only by use of Reynolds' transport theorem, Equation (5.18), in which the fluid property α is here the total energy per unit volume $\left(\rho e + \frac{1}{2}\rho \mathbf{v} \cdot \mathbf{v} \right)$. The resulting integro-differential equation is

$$\int_\Omega \left\{ \frac{\partial}{\partial t}\left(\rho e + \frac{1}{2}\rho \mathbf{v} \cdot \mathbf{v} \right) + \frac{\partial}{\partial r_k}\left[\left(\rho e + \frac{1}{2}\rho \mathbf{v} \cdot \mathbf{v} \right) v_k \right] \right\} d\Omega$$
$$= \int_S \mathbf{v} \cdot \mathbf{P} dS + \int_\Omega \mathbf{v} \cdot \rho f d\Omega - \int_S \mathbf{q} \cdot \mathbf{n} dS \quad (5.19)$$

The next step is to convert the two surface integrals into volume integrals so that the arbitrariness of Ω may be exploited to obtain a differential equation only. Using the fact that the force vector P is related to the stress tensor σ_{ij} by the equation $P_j = \sigma_{ij}n_i$, as was shown in the previous section, the first surface integral may be converted to a volume integral as follows:

$$\int_S \mathbf{v} \cdot \mathbf{P} dS = \int_S v_j \sigma_{ij} n_i dS = \int_\Omega \frac{\partial}{\partial x_i}\left(v_j \sigma_{ij} \right) d\Omega. \quad (5.20)$$

Gauss' theorem may be applied directly to the heat-flux term to give

$$\int q \cdot n\, dS = \int q_j n_j\, dS = \int_\Omega \frac{\partial q_j}{\partial x_j} d\Omega .$$

(5.21)

Since the stress tensor σ_{ij} has been brought into the energy equation, it is necessary to use the tensor notation from this point on. Then the expression for conservation of energy becomes

$$\int_\Omega \left\{ \frac{\partial}{\partial t}\left(\rho e + \frac{1}{2}\rho v_j v_j\right) + \frac{\partial}{\partial r_k}\left[\left(\rho e + \frac{1}{2}\rho v_j v_j\right)v_k\right]\right\} d\Omega$$
$$= \int_\Omega \frac{\partial}{\partial r_i}\left(v_j \sigma_{ij}\right) d\Omega + \int_\Omega v_j \rho f_j\, d\Omega - \int_\Omega \frac{\partial q_j}{\partial r_j} d\Omega$$

(5.22)

Having converted each term to volume integrals, the conservation equation may be considered to be of the form $\int_\Omega \{ \ \} d\Omega = 0$, where the choice of Ω is arbitrary. Then the quantity inside the brackets in the integrand must be zero, which results in the following differential equation:

$$\frac{\partial}{\partial t}\left(\rho e + \frac{1}{2}\rho v_j v_j\right) + \frac{\partial}{\partial r_k}\left[\left(\rho e + \frac{1}{2}\rho v_j v_j\right)v_k\right] = \frac{\partial}{\partial r_i}\left(v_j \sigma_{ij}\right) + v_j \rho f_j - \frac{\partial q_j}{\partial r_j} \quad (5.23)$$

This equation may be made considerably simpler by using the equations which have been already derived, as will now be demonstrated. The first term on the left-hand side may be expanded by considering ρe and $\frac{1}{2}\rho v_j v_j$ to be the products $(\rho)(e)$ and $(\rho)\left(\frac{1}{2}v_j v_j\right)$, respectively. Then

$$\frac{\partial}{\partial t}\left(\rho e + \frac{1}{2}\rho v_j v_j\right) = \rho\frac{\partial e}{\partial t} + e\frac{\partial \rho}{\partial t} + \rho\frac{\partial}{\partial t}\left(\frac{1}{2}v_j v_j\right) + \frac{1}{2}v_j v_j\frac{\partial \rho}{\partial t} \qquad (5.24)$$

Similarly, the second term on the left-hand side of the basic equation may be expanded by considering $\rho e v_k$ to be the product $(e)(\rho v_k)$ and $\frac{1}{2}\rho v_j v_j v_k$ to be the product $\left(\frac{1}{2}v_j v_j\right)(\rho v_k)$. Thus the equation becomes:

$$\frac{\partial}{\partial r_k}\left[\left(\rho e + \frac{1}{2}\rho v_j v_j\right)v_k\right] =$$

$$e\frac{\partial}{\partial r_k}(\rho v_k) + \rho v_k\frac{\partial e}{\partial r_k} + \frac{1}{2}v_j v_j\frac{\partial}{\partial r_k}(\rho v_k) + \rho v_k\frac{\partial}{\partial r_k}\left(\frac{1}{2}v_j v_j\right) \qquad (5.25)$$

In this last equation, the quantity $(\partial/\partial r_k)(\rho v_k)$, which appears in the first and third terms on the right-hand side, may be replaced by $-\partial\rho/\partial t$ in view of the continuity equation (5.6). Hence it follows that

$$\frac{\partial}{\partial r_k}\left[\left(\rho e + \frac{1}{2}\rho v_j v_j\right)v_k\right] = -e\frac{\partial \rho}{\partial t} + \rho v_k\frac{\partial e}{\partial r_k} - \frac{1}{2}v_j v_j\frac{\partial \rho}{\partial t} + \rho v_k\frac{\partial}{\partial r_k}\left(\frac{1}{2}v_j v_j\right) \qquad (5.26)$$

Now when the two components constituting the left-hand side of the basic conservation equation are added, the two terms with minus signs above are cancelled by corresponding terms with plus signs to give

$$\frac{\partial}{\partial t}\left(\rho e + \frac{1}{2}\rho v_j v_j\right) + \frac{\partial}{\partial r_k}\left[\left(\rho e + \frac{1}{2}\rho v_j v_j\right)v_k\right]$$

$$= \rho\frac{\partial e}{\partial t} + \rho v_k\frac{\partial e}{\partial r_k} + \rho\frac{\partial}{\partial t}\left(\frac{1}{2}v_j v_j\right) + \rho v_k\frac{\partial}{\partial r_k}\left(\frac{1}{2}v_j v_j\right)$$

$$= \rho\frac{\partial e}{\partial t} + \rho v_k\frac{\partial e}{\partial r_k} + \rho v_j\frac{\partial v_j}{\partial t} + \rho v_j v_k\frac{\partial v_j}{\partial r_k} \tag{5.27}$$

Then, noting that

$$\frac{\partial}{\partial r_i}\left(v_j\sigma_{ij}\right) = v_j\frac{\partial\sigma_{ij}}{\partial r_i} + \sigma_{ij}\frac{\partial v_j}{\partial r_i} \tag{5.28}$$

the equation which expresses the conservation of energy becomes

$$\rho\frac{\partial e}{\partial t} + \rho v_k\frac{\partial e}{\partial r_k} + \rho v_j\frac{\partial v_j}{\partial t} + \rho v_j v_k\frac{\partial v_j}{\partial r_k} = v_j\frac{\partial\sigma_{ij}}{\partial r_i} + \sigma_{ij}\frac{\partial v_j}{\partial r_i} + v_j\rho f_j - \frac{\partial q_j}{\partial r_j}. \tag{5.29}$$

Now it can be seen that the third and fourth terms on the left-hand side are cancelled by the first and third terms on the right-hand side, since these terms collectively amount to the product of v_j with the momentum Equation (5.16). Thus the equation which expresses conservation of thermal energy becomes

$$\rho\frac{\partial e}{\partial t} + \rho v_k\frac{\partial e}{\partial r_k} = \sigma_{ij}\frac{\partial v_j}{\partial r_i} - \frac{\partial q_j}{\partial r_j} \tag{5.30}$$

The terms which were dropped in the last simplification were the mechanical-energy terms. The equation of conservation of momentum, Equation (5.16), may be regarded as an equation of balancing forces with j as the free subscript. Therefore, the scalar product

of each force with the velocity vector, or the multiplication by v_j, gives the rate of doing work by the mechanical forces, which is the mechanical energy. On the other hand, Equation (5.30) is a balance of thermal energy, which is what is left when the mechanical energy is subtracted from the balance of total energy, and is usually referred to as simply the *energy equation*.

As was the case with the equation of momentum conservation, it is instructive to interpret each of the terms appearing in Equation (5.30) physically. The entire left-hand side represents the rate of change of internal energy, the first term being the temporal change while the second is due to local convective changes caused by the fluid flowing from one area to another. The entire right-hand side represents the cause of the change in internal energy. The first of these terms represents the conversion of mechanical energy into thermal energy due to the action of the surface stresses. As will be seen later, part of this conversion is reversible and part is irreversible. The final term in the equation represents the rate at which heat is being added by conduction from outside.

6. INCOMPRESSIBLE NAVIER-STOKES AND MAGNETO-HYDRODYNAMIC EQUATIONS

The Navier-Stokes (NS) equations for a conductive fluid are given by the following continuity, momentum, and energy equations:

$$\nabla \cdot \mathbf{V} = 0 \tag{6.1}$$

$$\rho \left[\frac{\partial \mathbf{V}}{\partial t} + \mathbf{V} \cdot \nabla \mathbf{V} \right] + \nabla P = \mu \nabla^2 \mathbf{V} + \rho \mathbf{g} + \mathbf{F}_{EM} \tag{6.2}$$

$$\rho C_v \left(\frac{\partial T}{\partial t} + u \frac{\partial T}{\partial x} + v \frac{\partial T}{\partial y} \right) = k \nabla^2 T + \frac{\mathbf{J}^T \cdot \mathbf{J}^T}{\sigma} \tag{6.3}$$

where ρ is the density, $\mathbf{V}$ is the velocity, P is the pressure, T is the temperature, μ and $\mathbf{g} = -g\hat{e}_y$ are viscosity and gravitational acceleration respectively, C_v is the specific heat, k and σ are thermal and electrical conductivities. And $\mathbf{F}_{EM}$ is the Lorentz force given by

$$\mathbf{F}_{EM} = \rho_e \mathbf{E}^T + \mathbf{J}^T \times \mathbf{B}^T \tag{6.4}$$

where ρ_e is the charge density, $\mathbf{E}^T, \mathbf{B}^T$ are total electric and magnetic fields and $\mathbf{J}^T$ is the total current density. Note that the last term in Equation (6.3) denotes the Joule heating due to the currents. Since the fluid is conductive, the NS equations must be accompanied with the Maxwell's equations given as:

$$\nabla \times \mathbf{E} = -\frac{\partial \mathbf{B}}{\partial t} \tag{6.5}$$

$$\nabla \times \mathbf{B} = \mu_0 \mathbf{J} + \mu_0 \varepsilon_0 \frac{\partial \mathbf{E}}{\partial t} \approx \mu_0 \mathbf{J} \tag{6.6}$$

$$\nabla \cdot \mathbf{E} = \frac{\rho_e}{\varepsilon_0} \approx 0 \tag{6.7}$$

$$\nabla \cdot \mathbf{B} = 0 \tag{6.8}$$

where $\mathbf{E}$ is the internal electric field, ρ_e is the internal charge density which is ignored since it is assumed that there is no charge seperation in the fluid. In that case the Lorentz force reduces to $\mathbf{F}_{EM} = \mathbf{J}^T \times \mathbf{B}^T$. In addition, ε_0 and μ_0 are the dielectric constant and magnetic permeability respectively. The magnetic and electric fields in Equations (6.5,6.6,6.7, and 6.8) are internal and induced fields and the term with the time rate of the electric field represents the displacement current (when the high frequency phenomena are ignored, this term is very small comparing with others, thus it is neglected). In the present problem, the external magnetic and electric fields are considered to be time-independent. When the system is assumed to be under the influence of such external electric and magnetic fields, one must guarantee that these fields satisfy the following stationary Maxwell's equations:

$$\nabla \times \mathbf{E}^{ext} = 0, \quad \nabla \cdot \mathbf{E}^{ext} = \frac{\rho_{ext}}{\varepsilon_0}, \nabla \times \mathbf{B}^{ext} = \mu_0 \mathbf{J}_{ext}^T, \quad \nabla \cdot \mathbf{B}^{ext} = 0 \tag{6.9}$$

Note that, NS and Maxwell's equations are coupled through the current density and charge. These are related by means of the following equation of charge conservation:

$$\frac{\partial q}{\partial t} + \nabla \cdot \mathbf{J} = 0 \quad , \quad \frac{\partial q_{ext}}{\partial t} + \nabla \cdot \mathbf{J}_{ext} = 0 . \tag{6.10}$$

Notice that the divergence of Equation (6.6) yields $\nabla \cdot \mathbf{J} = 0$ thus the internal and external charges are assumed to be constant in time.(i.e;Equation (6.10) leads to $\nabla \cdot \mathbf{J} = 0; \nabla \cdot \mathbf{J}_{ext} = 0$).

The current density and electric field are related in the local rest frame ® of the fluid by Ohm's Law:

$$\mathbf{J}^{\mathbf{R}} = \sigma \mathbf{E}^{\mathbf{R}} \tag{6.11}$$

since fluid is incompressible (v<<c; speed of light) the laboratory and rest frame values are related by;

$$\mathbf{J}^{\mathbf{R}} = \mathbf{J} - \rho_e \mathbf{V} \approx \mathbf{J}, \tag{6.12}$$

$$\mathbf{F}_{\mathbf{EM}} = \rho_e \mathbf{E}^{\mathbf{T}} + \mathbf{J}^{\mathbf{T}} \times \mathbf{B}^{\mathbf{T}}. \tag{6.13}$$

If Equations (6.11 and 6.13) are combined the obtained equations would be like:

$$\mathbf{J} = \sigma(\mathbf{E} + \mathbf{V} \times \mathbf{B}) = \frac{\nabla \times \mathbf{B}}{\mu_0}, \mathbf{J}_{ext} = \sigma(\mathbf{E}^{ext} + \mathbf{V} \times \mathbf{B}_{ext}) = \frac{\nabla \times \mathbf{B}^{ext}}{\mu_0}. \tag{6.14}$$

Since the internal charge density in Lorentz Force is ignored the current density becomes: $\mathbf{J}^T = (\nabla \times (\mathbf{B} + \mathbf{B}_{ext}))/\mu_0$.

Thus the x and y components of momentum equations in two dimensions become:

$$\frac{\partial u}{\partial t} + u\frac{\partial u}{\partial x} + v\frac{\partial u}{\partial y} + \frac{1}{\rho}\frac{\partial P}{\partial x} + \frac{B_y}{\rho\mu_0}\left(\frac{\partial B_y}{\partial x} - \frac{\partial B_x}{\partial y}\right) = \nu\nabla^2 u - \frac{B_y^{ext}}{\rho\mu_0}\left(\frac{\partial B_y^{ext}}{\partial x} - \frac{\partial B_x^{ext}}{\partial y}\right) \tag{6.15}$$

$$\frac{\partial v}{\partial t} + u\frac{\partial v}{\partial x} + v\frac{\partial v}{\partial y} + \frac{1}{\rho}\frac{\partial P}{\partial y} - \frac{B_x}{\rho\mu_0}\left(\frac{\partial B_y}{\partial x} - \frac{\partial B_x}{\partial y}\right) = \nu\nabla^2 v - g + \frac{B_x^{ext}}{\rho\mu_0}\left(\frac{\partial B_y^{ext}}{\partial x} - \frac{\partial B_x^{ext}}{\partial y}\right). \tag{6.16}$$

Since the electric field is given (see Equation (6.14)) by;

$$\mathbf{E} = (\mathbf{J}/\sigma) - (\mathbf{V} \times \mathbf{B}) = [(\nabla \times \mathbf{B})/\mu_0 \sigma] - \mathbf{V} \times \mathbf{B}, \tag{6.17}$$

The Faraday's Law given by Equation (6.5) becomes:

$$\frac{\partial \mathbf{B}}{\partial t} - \nabla \times (\mathbf{V} \times \mathbf{B}) = -\frac{\nabla^2 \mathbf{B}}{\mu_0 \sigma} \tag{6.18}$$

since $\nabla \times (\nabla \times \mathbf{B}) = -\nabla^2 \mathbf{B}$ because $\nabla \cdot \mathbf{B} = 0$. For the fluid under consideration, this has the form as diffusion equation. It is noted that when the fluid is highly conductive the characteristic time scale for the induced transient magnetic field gets longer (high magnetic Reynold's number). Thus the magnetic field lines are said to be frozen in not fully diffused in the fluid. In two dimensions, the Faraday's Law can be written as;

$$\frac{\partial B_x}{\partial t} + B_x \frac{\partial v}{\partial y} - u \frac{\partial B_y}{\partial y} - B_y \frac{\partial u}{\partial y} + v \frac{\partial B_x}{\partial y} = \frac{1}{\mu_0 \sigma} \nabla^2 B_x \tag{6.19}$$

$$\frac{\partial B_y}{\partial t} + B_y \frac{\partial u}{\partial x} - v \frac{\partial B_x}{\partial x} - B_x \frac{\partial v}{\partial x} + u \frac{\partial B_y}{\partial x} = \frac{1}{\mu_0 \sigma} \nabla^2 B_y. \tag{6.20}$$

Equations (6.19 and 6.20) are not symmetric and creates difficulties in determining the eigen-system of the equation set. Thus the terms: $-\mathbf{V}\nabla \cdot \mathbf{B}$ and $\mathbf{B}\nabla \cdot \mathbf{V}$ are added to the rhs of Equation (6.19). So that not only the equation set is made symmetric but also numerical errors due to divergence conditions are eliminated. In that case Faraday's Law turns into:

$$\frac{\partial B_x}{\partial t} - B_x \frac{\partial u}{\partial x} + u \frac{\partial B_x}{\partial x} - B_y \frac{\partial u}{\partial y} + v \frac{\partial B_x}{\partial y} = \frac{1}{\mu_0 \sigma} \nabla^2 B_x \tag{6.21}$$

$$\frac{\partial B_y}{\partial t} - B_y \frac{\partial v}{\partial y} - v \frac{\partial B_y}{\partial y} - B_x \frac{\partial v}{\partial x} + u \frac{\partial B_y}{\partial x} = \frac{1}{\mu_0 \sigma} \nabla^2 B_y. \tag{6.22}$$

By using the Ohm's Law (i.e.; $\mathbf{J} = \rho(\mathbf{E} + \mathbf{V} \times \mathbf{B})$) the energy equation becomes:

$$\frac{\partial T}{\partial t} + u\frac{\partial T}{\partial x} + v\frac{\partial T}{\partial y} = \frac{k}{\rho C_v}\nabla^2 T + \frac{\sigma\left|\mathbf{V} \times \mathbf{B}\right|^2}{\rho C_v} + \frac{\sigma E_{ext}^2}{\rho C_v} + \frac{\sigma\left|\mathbf{V} \times \mathbf{B}^{ext}\right|^2}{\rho C_v} \quad . \quad (6.23)$$

where $\mathbf{E} \approx 0$ was considered since $\dfrac{\partial \mathbf{E}}{\partial t} = 0$, $\nabla \cdot \mathbf{E} = 0$ and $\rho_e \cong 0$ so that the current density balances $\mathbf{V} \times \mathbf{B}$ currents so that $\mathbf{E} = \dfrac{\mathbf{J}}{\rho} - \mathbf{V} \times \mathbf{B} \approx 0$. Since $\mathbf{V} \times \mathbf{B} = \left(uB_y - vB_x\right)\hat{e}_z$, this equation can be written as:

$$\frac{\partial T}{\partial t} + v\frac{\partial T}{\partial x} + v\frac{\partial T}{\partial y} = \frac{k}{\rho C_v}\nabla^2 T + \frac{\sigma\left(uB_y - vB_x\right)^2}{\rho C_v} + \frac{\sigma\left(uB_y^{ext} - vB_x^{ext}\right)^2}{\rho C_v} + \frac{\sigma E_{ext}^2}{\rho C_v} . \quad (6.24)$$

Notice that the existence of external magnetic and electric fields have a positive effect in temperature increase.

6.1. Artificial Compressibility and Monopole Function

Major advances in the state of the art in CFD (Computational Fluid Dynamics) have been made in conjunction with compressible flow computations. Therefore, it is of significant interest to be able to use some of these compressible flow algorithms for incompressible flows. To do this,the artificial compressibility method of Chorin (1967) can be used. In this formulation, the continuity equation is modified by adding a pseudo-time derivative of the pressure,resulting in

$$\frac{1}{\beta}\frac{\partial P}{\partial \tau} + \frac{\partial u_i}{\partial x_i} = 0 \quad\quad\quad (6.25)$$

where β is an artificial compressibility parameter and τ is a pseudo-time parameter.This forms a hyperbolic-parabolic type of pseudo-time dependent system of equations. Thus, implicit schemes developed for compressible flows can be implemented to solve for steady-state solution. In the steady-state formulation the equations are to be marched in a time-like fashion until the divergence of velocity in equation (6.25) converges to a specified tolerance. The time variable for this process no longer represents physical time, so in the momentum equations t is replaced with τ, which can be thought of as a pseudo-time or iteration parameter.

Physically, this means that waves of finite speed are introduced into the incompressible flow field as a medium to distribute the pressure. For a truly incompressible flow, the wave speed is infinite,whereas the speed of propagation of these pseudo waves depend on the magnitude of the artificial compressibility parameter. In a truly incompressible flow, the pressure field is affected instantaneously by a disturbance in the flow, but with artificial compressibility, there is a time lag between the flow disturbance and its effect on the pressure field. Ideally, the value of the artificial compressibility parameter is to be chosen as high as the particular choice of algorithm will allow so that the incompressibility is recovered quickly. This has to be done without lessening the accuracy and the stability property of the numerical method implemented. On the other hand, if the artificial compressibility parameter is chosen such that these waves travel too slowly, then the variation of the pressure field accompanying these waves is very slow. This will interfere with the proper development of the viscous boundary layer. In viscous flows, the behavior of the boundary layer is very sensitive to the streamwise pressure gradient, especially when the boundary layer is separated. If separation is present, a pressure wave travelling with finite speed will cause a change in the local pressure gradient which will affect the location of the flow separation. This change in separated flow will feed back to the pressure field, possibly preventing convergence to a steady state. When the viscous effect is important for the entire flow field as in most internal flow problems, the interaction between the pseudo-pressure waves and the viscous flow field is especially important.

Artificial compressibility relaxes the strict requirement of satisfying mass conservation in each step. However, to utilize this convinient feature, it is essential to

understand the nature of the artificial compressibility both physically and mathematically. Chang and Kwak (1984) reported details of the artificial compressibility, and suggested some guidelines for choosing the artificial compressibility parameter. Various applications which evolved from this concept have been reported for obtaining steady-state solutions (e.g., Steger and Kutler, 1977; Kwak et al. 1986; Chang et al. 1988; Choi and Merkle, 1985). To obtain time-dependent solutions using this method, an iterative procedure can be applied in each physical time step such that the continuity equation is satisfied (see, Merkle and Athavale, 1987, Rogers and Kwak, 1988, Rogers, Kwak and Kiris, 1991, Belov et al. 1995). Further discussions on the artificial compressibility approach can be found in the literature (see, Temam, 1979, Rizzi and Eriksson, 1985).

Combining equation (6.25) and the momentum equations gives the following system of equations:

$$\frac{\partial}{\partial \tau}\hat{D} = -\frac{\partial}{\partial \zeta_i}\left(\hat{E}_i - \hat{E}_{vi}\right) + \hat{S} = -\hat{R} \qquad (6.26)$$

where R is the right-hand-side of the momentum equation and can be defined as the residual for steady-state computations, and where

$$\hat{D} = \frac{D}{J} = \frac{1}{J}\begin{bmatrix} p \\ u \\ v \\ w \end{bmatrix}, \qquad \hat{E}_i = \begin{bmatrix} \beta U_i \iota J \\ \hat{e}_i \end{bmatrix}, \qquad \hat{E}_{vi} = \begin{bmatrix} 0 \\ \hat{e}_{vi} \end{bmatrix}. \qquad (6.27)$$

When the governing equations are solved in a steadily rotating reference frames, the source term, $\hat{S}$, represents centrifugal and Coriolis terms. If the relative reference frame is rotating around the x-axis, the source term $\hat{S}$ is given by

$$\hat{S} = \begin{bmatrix} 0 \\ 0 \\ \Omega(\Omega y + 2w) \\ \Omega(\Omega z - 2v) \end{bmatrix} \qquad (6.28)$$

where Ω is the rotational speed. In this report, the source term, $\hat{S}$, is set to zero other than for rotational steady solutions. Relative velocity components are written in terms of absolute velocity components u_a, v_a, and w_a as

$$u = u_a, \qquad v = v_a + \Omega z, \qquad w = w_a - \Omega y.$$ (6.29)

Time-dependent calculation of incompressible flows are especially time consuming due to the eliptic nature of the governing equations. This means that any local change in the flow has to be propagated throughout the entire flow field. Numerically, this means that in each time step, the pressure field has to go through one complete steady-state iteration cycle, for example, by Poisson-solver-type pressure iteration or artificial compressibility iteration method. In transient flow, the physical time step has to be small and consequently the change in the flow field may be small. In this situation, the number of iterations in each time step for getting a divergence-free flow field may not be as high as regular steady-state computations. However, the time- accurate computations are generally an order of magnitude more time-consuming than steady-state computation. Therefore, it is particularly desirable to develope computationally efficient methods either by implementing a fast algorithm and by utilizing computer characteristics such as vectorization and parallel processing.

A time-accurate method using artificial compressibility developed by Rogers, Kwak, and Kiris (1991) is summarized next. In this formulation the time derivatives in the momentum equations are differenced using a second-order, three-point, backward-difference formula;

$$\frac{3\tilde{u}^{n+1} - 4\tilde{u}^n + \tilde{u}^{n-1}}{2\Delta t} = -\hat{r}^{n+1}$$ (6.30)

where the superscript n denotes the quantities at time $t = n\Delta t$ and $\hat{r}$ is the right-hand side given in equation;

$$\frac{\partial}{\partial t}\hat{u} = -\frac{\partial}{\partial \xi_i}\left(\hat{e}_i - \hat{e}_{vi}\right) + \hat{s} = -\hat{r}.\tag{6.31}$$

To solve equation (6.30) for a divergence free velocity field at the $(n+1)$ time level, a pseudo-time level is introduced and is denoted by a superscript m. The equations are iteratively solved such that $\hat{u}^{n+1,m+1}$ approaches the new velocity $\hat{u}^{n+1}$ as the divergence of $\hat{u}^{n+1,m+1}$ approaches zero. To drive the divergence of this velocity to zero, the following artificial compressibility relation is introduced:

$$\frac{p^{n+1,m+1} - p^{n+1,m}}{\Delta \tau} = -\beta \nabla \cdot \hat{u}^{n+1,m+1}\tag{6.32}$$

where τ denotes pseudo-time and β is an artificial compressibility parameter. Combining equation (6.32) with the momentum equations gives;

$$I_{tr}\left(\hat{D}^{n+1,m+1} - \hat{D}^{n+1,m}\right) = -\hat{R}^{n+1,m+1} - \frac{I_m}{\Delta t}\left(1.5\hat{D}^{n+1,m} - 2\hat{D}^n + 0.5\hat{D}^{n-1}\right)\tag{6.33}$$

where $\hat{D}$ is the same vector defined in equation (6.30), $\hat{R}$ is the same residual vector defined in equation (6.26), and I_{tr} is a diagonal matrix given by;

$$I_{tr} = diag\left[\frac{1}{\Delta t}, \frac{1.5}{\Delta t}, \frac{1.5}{\Delta t}, \frac{1.5}{\Delta t}\right].\tag{6.34}$$

Finally, the residual term at the m+1 pseudo-time level is solved by multistage Runga-Kutta algorithm. The MHD equations (Eqs.6.1, 6.15, 6.16, 6.20, 6.21, 6.24) derived here are used for incompressible flows, so that the divergence constraints for velocity and magnetic field (i.e., $\nabla \cdot \mathbf{V} = 0$, $\nabla \cdot \mathbf{B} = 0$) should be satisfied. In this work, these conditions are modified to read as;

$$\frac{\partial P}{\partial \tau} + \beta^2 \nabla \cdot \mathbf{V} = 0 \qquad\qquad (6.35)$$

$$\frac{\partial \psi}{\partial \tau} + \alpha^2 \nabla \cdot \mathbf{B} = 0 \qquad\qquad (6.36)$$

where τ is the pseudo-time step, β^2 is the artificial compressibility parameter, α^2 is the artificial magnetic monopole parameter and ψ is the magnetic monopole function which is used to correct the magnetic fields. These equations are solved as sub-iterations between each time step to force the velocity and magnetic fields to satisfy the divergence constraints. As sub-iterations converge (i.e., $\partial/\partial \tau \rightarrow 0$), P and ψ relax to the necessary values which will be able to correct the velocity and magnetic fields in such a way that the divergence conditions are satisfied.

Note that the artificial compressibility parameter were first introduced in [9] and the magnetic monopole equation, Equation (6.36), is similar to that is given in [9]and this procedure is called the relaxation scheme. In order relaxation scheme to fix the magnetic fields, the corrective effect of ψ is introduced into the Faraday's equation by inserting the terms: $\partial\psi/\partial x$ and $\partial\psi/\partial y$ into Equations (6.20, 6.21) respectively [9]

In order this procedure to be consistent, with the relaxation scheme described here, it can be shown that the term: $[(B_x/\rho C_v)(\partial\psi/\partial x) + (B_y/\rho C_v)(\partial\psi/\partial y)]$ should be added to the left hand side of the energy equation, Equation (6.24).

By considering all the derivations so far, the resulting MHD equations including the effects of ψ turn into the following equation set:

$$\frac{\partial P}{\partial \tau} + \beta^2 \nabla \cdot \mathbf{V} = 0, \quad \frac{\partial \psi}{\partial \tau} + \alpha^2 \nabla \cdot \mathbf{B} = 0 \qquad\qquad (6.37)$$

$$\frac{\partial u}{\partial t} + u\frac{\partial u}{\partial x} + v\frac{\partial u}{\partial y} + \frac{1}{\rho}\frac{\partial P}{\partial x} + \frac{B_y}{\rho\mu_0}\left(\frac{\partial B_y}{\partial x} - \frac{\partial B_x}{\partial y}\right) = \nu\nabla^2 u - \frac{B_y^{ext}}{\rho\mu_0}\left(\frac{\partial B_y^{ext}}{\partial x} - \frac{\partial B_x^{ext}}{\partial y}\right) \quad (6.38)$$

$$\frac{\partial v}{\partial t} + u\frac{\partial v}{\partial x} + v\frac{\partial v}{\partial y} + \frac{1}{\rho}\frac{\partial P}{\partial y} - \frac{B_x}{\rho\mu_0}\left(\frac{\partial B_y}{\partial x} - \frac{\partial B_x}{\partial y}\right) =$$
$$\nu\nabla^2 v + \frac{B_x^{ext}}{\rho\mu_0}\left(\frac{\partial B_y^{ext}}{\partial x} - \frac{\partial B_x^{ext}}{\partial y}\right) - g \quad (6.39)$$

$$\frac{\partial B_x}{\partial t} - B_x\frac{\partial u}{\partial x} + u\frac{\partial B_x}{\partial x} - B_y\frac{\partial u}{\partial y} + v\frac{\partial B_x}{\partial y} + \frac{\partial \psi}{\partial x} = \frac{1}{\mu_0\sigma}\nabla^2 B_x \quad (6.40)$$

$$\frac{\partial B_y}{\partial t} - B_y\frac{\partial v}{\partial y} - v\frac{\partial B_y}{\partial y} - B_x\frac{\partial v}{\partial x} + u\frac{\partial B_y}{\partial x} + \frac{\partial \psi}{\partial y} = \frac{1}{\mu_0\sigma}\nabla^2 B_y \quad (6.41)$$

$$\frac{\partial T}{\partial t} + u\frac{\partial T}{\partial x} + v\frac{\partial T}{\partial y} + \frac{B_x}{\rho C_v}\frac{\partial \psi}{\partial x} + \frac{B_y}{\rho C_v}\frac{\partial \psi}{\partial y} = \frac{k}{\rho C_v}\nabla^2 T +$$
$$\frac{\sigma}{\rho C_v}E_{ext}^2 + \frac{\sigma(uB_y - vB_x)^2}{\rho C_v} + \frac{\sigma(uB_y^{ext} - vB_x^{ext})^2}{\rho C_v} \quad (6.42)$$

Note that the continuity equation, Equation (6.1), states that the density is constant. However, when temperature gradients exist in the solution domain, the natural convection occurs with slight changes in the density. In this work, it is assumed that the density variations are very small so that the Boussinesq approximation holds. In this case, the density can be written as a function of temperature as follows:

$$\rho = \rho_\infty\left[1 - \beta(T - T_\infty)\right] \quad (6.43)$$

where ρ_∞ and T_∞ are ambient density and temperature (usually taken as outside parameters) and β is the expansion coefficient. Inserting this form of density to the right hand side of the momentum equations, and defining a new pressure as $P = P' + P_\infty$ (where $P' = P - P_\infty$ is the reduced pressure) the y component of the momentum equation becomes:

$$\frac{\partial v}{\partial t} + u\frac{\partial v}{\partial x} + v\frac{\partial v}{\partial y} + \frac{1}{\rho}\frac{\partial P'}{\partial y} - \frac{B_x}{\rho\mu_0}\left(\frac{\partial B_y}{\partial x} - \frac{\partial B_x}{\partial y}\right) = \nu\nabla^2 v + g\beta(T - T_\infty) \qquad (6.44)$$

For the energy equation, we define a new variable, $\theta = \dfrac{T - T_\infty}{\Delta T}$ where ΔT is the temperature difference and write the heat Equation (6.42) as follows:

$$\frac{\partial\theta}{\partial t} + u\frac{\partial\theta}{\partial x} + v\frac{\partial\theta}{\partial y} + \frac{B_x}{\mu_0\rho C_v\Delta T}\frac{\partial\psi}{\partial x} + \frac{B_y}{\mu_0\rho C_v\Delta T}\frac{\partial\psi}{\partial y} = \frac{k}{\rho C_v}\nabla^2\theta +$$
$$\frac{\sigma}{\rho C_v\Delta T}E_{ext}^2 + \frac{\Omega_m^2}{\rho C_v\sigma\mu_0^2\Delta T} + \frac{\sigma\left|V\times B^{ext}\right|^2}{\rho C_v\Delta T} \qquad . \qquad (6.45)$$

6.2. Dimensionless Form of MHD Equations

In this work, we use the following dimensionless parameters in order to write the dimension-less form of MHD equations:

$$x' = \frac{x}{L_0}, \quad t' = \frac{t}{t_0}, \quad P' = \frac{P}{P_0}, \quad \rho' = \frac{\rho}{\rho_\infty}, \quad B' = \frac{B}{B_0}, \quad \psi' = \frac{\psi}{\psi_0}, \quad E' = \frac{E}{E_0}, \quad V' = \frac{V}{V_0}$$

where the procedure of making the MHD equations dimensionless produces the following parameters:

$$\text{Reynold's Number} \qquad Re = L_0 V_0 / \nu \qquad (6.46)$$

$$\text{Interaction Parameter} \qquad N = \frac{\sigma B_0^2 L_0}{\rho_0 V_0} \qquad (6.47)$$

Magnetic Reynold's Number $\quad Re_m = \mu_0 \sigma V_0 L_0 = \dfrac{\mu_0 V_0 L_0}{\eta}$ $\qquad$ (6.48)

Hartmann Number $\qquad Ha = \sqrt{NR_e} = B_0 L_0 / \sqrt{\sigma / \mu}$ $\qquad$ (6.49)

Rayleigh Number $\qquad Ra = \dfrac{g\beta \Delta T L_0^3}{\upsilon \kappa}$ $\qquad$ (6.50)

Prandtl Number $\qquad Pr = \dfrac{\upsilon}{\kappa}, \quad \kappa = \dfrac{k}{\rho_0 C_v}$ $\qquad$ (6.51)

Eckert Number $\qquad E = \dfrac{V_0^2}{C_p \Delta T}.$ $\qquad$ (6.52)

Using these parameters, the dimensionless form of the MHD equations can be cast into:

$$\frac{\partial U}{\partial \tau} + I_m \frac{\partial U}{\partial t} + A \frac{\partial U}{\partial x} + B \frac{\partial U}{\partial y} = S_v + S^{ext} \qquad (6.53)$$

where $U = \lfloor P', u, v, \theta, B_x, B_y, \psi \rfloor$ is the state vector, $I_m = \mathrm{diag}[0,1,1,1,1,1,0]$ is the diagonal matrix, A and B are coefficient matrices of $\partial U / \partial x$ and $\partial U / \partial y$, and S_v, S^{ext} are viscous and external sources. This equation in detail is given below:

$$\frac{\partial}{\partial \tau}\begin{bmatrix} P' \\ u \\ v \\ \theta \\ B_x \\ B_y \\ \psi \end{bmatrix} + I_m \frac{\partial}{\partial t}\begin{bmatrix} P' \\ u \\ v \\ \theta \\ B_x \\ B_y \\ \psi \end{bmatrix} + \begin{bmatrix} 0 & \beta^2 & 0 & 0 & 0 & 0 & 0 \\ 1 & u & 0 & 0 & 0 & Y & 0 \\ 0 & 0 & u & 0 & 0 & -X & 0 \\ 0 & 0 & 0 & u & 0 & 0 & EB_x \\ 0 & -B_x^T & 0 & 0 & u & 0 & 1 \\ 0 & 0 & -B_x^T & 0 & 0 & u & 0 \\ 0 & 0 & 0 & 0 & \delta^2 & 0 & 0 \end{bmatrix}\frac{\partial}{\partial x}\begin{bmatrix} P' \\ u \\ v \\ \theta \\ B_x \\ B_y \\ \psi \end{bmatrix} +$$

$$\begin{bmatrix} 0 & 0 & \beta^2 & 0 & 0 & 0 & 0 \\ 0 & v & 0 & 0 & -Y & 0 & 0 \\ 0 & 0 & v & 0 & X & 0 & 0 \\ 0 & 0 & 0 & v & 0 & 0 & EB_y \\ 0 & -B_y^T & 0 & 0 & v & 0 & 0 \\ 0 & 0 & -B_y^T & 0 & 0 & v & 1 \\ 0 & 0 & 0 & 0 & 0 & \alpha^2 & 0 \end{bmatrix}\frac{\partial}{\partial y}\begin{bmatrix} P' \\ u \\ v \\ \theta \\ B_x \\ B_y \\ \psi \end{bmatrix} = \begin{bmatrix} 0 \\ 1/\mathrm{Re}\,\nabla^2 u \\ 1/\mathrm{Re}\,\nabla^2 v \\ 1/\mathrm{Re}\,\mathrm{Pr}\,\nabla^2 \theta \\ 1/\mathrm{Re}_m \nabla^2 B_x \\ 1/\mathrm{Re}_m \nabla^2 B_y \\ 0 \end{bmatrix} + \begin{bmatrix} 0 \\ S_2 \\ S_3 \\ S_4 \\ 0 \\ 0 \\ 0 \end{bmatrix} \qquad (6.54)$$

where

$$S_2 = \frac{-N}{\mathrm{Re}_m}B_y^{\mathrm{ext}}\left(\frac{\partial B_y^{\mathrm{ext}}}{\partial x} - \frac{\partial B_x^{\mathrm{ext}}}{\partial y}\right), \quad S_3 = \frac{N}{\mathrm{Re}_m}B_x^{\mathrm{ext}}\left(\frac{\partial B_y^{\mathrm{ext}}}{\partial x} - \frac{\partial B_x^{\mathrm{ext}}}{\partial y}\right) + \frac{\mathrm{Ra}\theta}{\mathrm{Pr}\,\mathrm{Re}^2} \qquad (6.55)$$

$$S_4 = NE\left[E_{\mathrm{ext}}^2 + \left(uB_y - vB_x\right)^2 + \left(uB_y^{\mathrm{ext}} - vB_x^{\mathrm{ext}}\right)^2\right] \quad \text{and} \quad X = \frac{NB_x}{\mathrm{Re}_m}, \; Y = \frac{NB_y}{\mathrm{Re}_m} \dots (6.56)$$

Note that the first and last elements of Equation (6.54) are exactly the same as Equations (6.35, 6.36) and that the time rates of P' and ψ are seperated from original equations by means of I_m.

6.3. Numerical Solution : Matrix Distribution Scheme

The incompressible MHD equations can be discretized by several discretization techniques (such as finite difference, finite volume, finite element etc.). In this work, a new method called "matrix distribution scheme" is used [10].

In this scheme, the discretized form of the system of MHD equations is obtained by integrating it over the area of a triangle, Ω_T, which has the nodes of i, j, k, see Figure 6.1.

$$\iint_{\Omega_T} \left(\frac{\partial \vec{U}}{\partial t} + A \frac{\partial \vec{U}}{\partial x} + B \frac{\partial \vec{U}}{\partial y} \right) d\Omega_T = \iint_{\Omega_T} \left(\vec{S}_v + \vec{S}^{ext} \right) d\Omega_T \qquad (6.57)$$
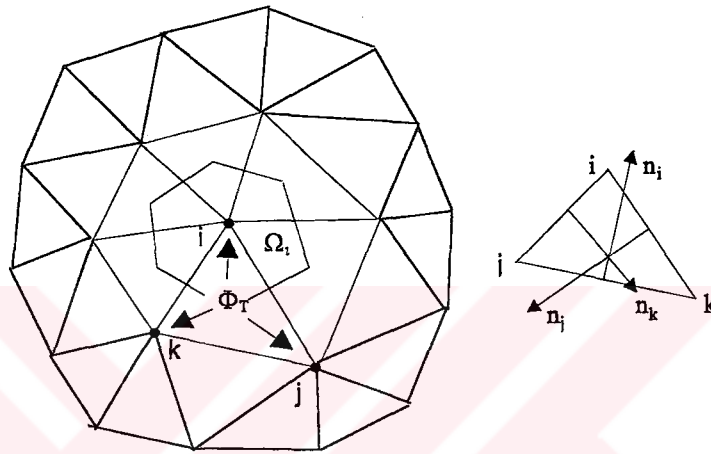

Figure.6.1. Triangular mesh structure showing the triangle area, Ω_T, the Veroni area, S_i, surrounding node: i, and the interior normals of a typical mesh: m.

By using forward difference formula for the time derivative and employing Gauss law for the convection terms on the left hand side of Equation (6.57), one obtains the following update formula at node "i" which is located at one of the vertices of triangle "T":

$$\frac{U_i^{n+1} - U_i^{n}}{\Delta t} \Omega_i + \oint_{\delta \ell_T} (A n_x + B n_y) U d\ell_T = (S_i^v + S_i^B) \Omega_T \qquad (6.58)$$

where Ω_i, is the Veroni area surrounding node i (see Figure.6.1) and Δt is the time interval. By using numerical trapezoidal method for the flux integral (contour integral in Equation 6.58) and considering all the triangles surrounding node i, Equation (6.58) can be written as:

$$\mathbf{U}_i^{n+1} = \mathbf{U}_i^n - \frac{\Delta t}{\Omega_i} \left[\sum_{\substack{triangles \\ around\ i}} \left(\Phi_i^T - \frac{\Omega_T (\mathbf{S}_i^v + \mathbf{S}_i^{ext})}{3} \right) \right] \tag{6.59}$$

for the state vector at the node "i" . As seen, the source terms are distributed equally among the nodes of "T" while Φ_i^T is the cell fluctuation (a fraction of total fluctuation Φ_T) assigned to the node "i" given by

$$\Phi_i^T = B_i \Phi^T = B_i \sum_{m=1}^{3} K_m \mathbf{U}_m . \tag{6.60}$$

where B_i is the distribution matrix which is responsible in determining how much of Φ_T should be distributed among the nodes of "T".

Here, $K_m = (An_x + Bn_y)_m/2$ is called the 2D Jacobian matrix (at node m=i, j, k of triangle T) and it is given by;

$$K_m = \begin{bmatrix} 0 & \beta^2 n_x & \beta^2 n_y & 0 & 0 & 0 & 0 \\ n_x & V_n & 0 & 0 & -\dfrac{NB_y}{R_{em}} n_y & \dfrac{NB_y}{R_{em}} n_x & 0 \\ 0 & 0 & V_n & 0 & \dfrac{NB_x}{R_{em}} n_y & -\dfrac{NB_x}{R_{em}} n_x & 0 \\ 0 & 0 & 0 & V_n & 0 & 0 & EB_n \\ 0 & -B_n^T & 0 & 0 & V_n & 0 & n_x \\ 0 & 0 & -B_n^T & 0 & 0 & V_n & n_y \\ 0 & 0 & 0 & 0 & \delta^2 n_x & \delta^2 n_y & 0 \end{bmatrix}_m \tag{6.61}$$

where n_x and n_y are the x and y components of the normal vectors (see Figure.6.1) whose magnitudes are equal to the associated side lengths, $V_T = un_x + vn_y$ is the tangential velocity

along streamlines. It should be noted here that the numerical integrations were performed by assuming that the state variables are assumed to vary linearly over the triangle.

The matrix B_i assumes the role of distributing appropriate fractions of the total fluctuation to the nodes of triangle. The different forms for B_i results in different methods all of which produce similar results. For example, when $B_i=I/3$, where I is the unit matrix, the method is called classical Galerkin Finite Element method which has some stability problems. In the method presented here, the classical second order accurate Lax-Wendroff method is used such that the distribution matrix (Galerkin form plus extra dissipation) is defined

$$B_i = \frac{1}{3}I + \frac{\Delta t_T}{2S_i} K_i^T \qquad (6.62)$$

where "Δt_T" is a characteristic local time step for the triangle considered and the second term is extra numerical dissipation. It is noted that, the careful design of this matrix is very important for numerical accuracy and that regardless of the method used, the distribution matrices on the nodes of "T" should satisfy the following property for consistency:

$$B_i + B_j + B_k = I . \qquad (6.63)$$

When the updating procedure is performed triangle by triangle, the updating formula given by Equation (6.59) turns into the following update at node i due to the triangle T:

$$U_i^{n+1} \leftarrow U_i^n - \frac{\Delta t}{\Omega_i}\left[\Phi_i^T - \Omega_T(S_i^Y + S_i^B)\right] + tfot \qquad (6.64)$$

where "tfot" represents the terms from other triangles surrounding node "i". When all triangles are visited and their associated fluctuations are distributed to their nodes by

means of the distribution matrix, all the nodes in the mesh will have been updated at new time step.

6.4.   Temporal Discretization:Dual Time Stepping

The incompressible system given by is very stiff numerically since the ratio of the convection speed to the speed of sound is very small. To overcome this difficulty, preconditioning techniques can be used to carefully alter the time evolution of the equations. If the preconditioning is applied to real time advancements, the time evolution loses its meaning turning into just some iterations to reach the steady-state. If the time accurate (transient) solutions are seeked, then this procedure must be applied as pseudo iterations at each real time step. To do this,

$$P\frac{\partial U}{\partial \tau}+I_m\frac{\partial U}{\partial t}+A\frac{\partial U}{\partial x}+B\frac{\partial U}{\partial y}=S_v+S^{ext/int} \qquad (6.65)$$

where P is the preconditioning matrix and τ is the pseudo-time. Different forms of P exist in literature, but here a simple form given by $P=diag\left[\frac{1}{\beta^2},1,1,1,1\right]$ is used. Upon multiplying Equation (6.65) by the inverse of P, the preconditioned system can be written as:

$$\frac{\partial U}{\partial \tau}+I_m\frac{\partial U}{\partial t}+A\left(\beta^2\right)\frac{\partial U}{\partial x}+B\left(\beta^2\right)\frac{\partial U}{\partial y}=S_v+S^{ext/int} \qquad (6.66)$$

where this operation did not change the sources and time evolution of U but only modified the continuity equation by changing only the first row elements of matrices A and B (i.e., 1s in the first row are replaced by β^2, artificial compressibility parameter). Actually, this

procedure is nothing but modifying the divergence condition to employ an artificial equation for pressure to be advanced in pseudo-time:

$$\frac{\partial P^*}{\partial t} = -\beta^2 \nabla \cdot V \tag{6.67}$$

in order to drive the velocity divergence to zero before the new time level is reached. Note that, in numerical time derivatives it is better to utilize implicit time stepping by Newton type algorithm. But this method is very complicated for unstructured triangular grids. That's why the pseudo-time iterations in this work were carried out by explicit multistage Runga-Kutta algorithm in which the pseudo-time step must be carefully found by the spectral radii of $P^{-1}(A,B)$ as $\Delta\tau = \dfrac{CFL}{\lambda_{max}/L}$ where λ is the eigenvalue of $P^{-1}(A,B)$ and L is minimum cell length. When this modified equation system reaches steady-state in pseudo-time $\left(\dfrac{\partial U}{\partial \tau} \to 0\right)$, the time accurate solution is recovered;

$$I_m \frac{\partial U}{\partial t} = \mathrm{Re}\, s(U,P) \tag{6.68}$$

Where

$$\mathrm{Re}\, s(U,P) = -A(\beta^2)\frac{\partial U}{\partial x} - B(\beta^2)\frac{\partial U}{\partial y} + S_v + S_{ext} \tag{6.69}$$

is called preconditioned residual vector. As done in (?), the real time derivative is approximated by the following 3-level formula;

$$\frac{\partial U}{\partial t} = \frac{1+\phi}{\Delta t}\left(U^{n+1} - U^n\right) - \frac{\phi}{\Delta t}\left(U^n - U^{n-1}\right) \tag{6.70}$$

where $\phi = 0$ gives explicit first order while $\phi = 0.5$ (this was used in this work) gives the second order accuracy in time. By combining the real time levels with those of the pseudo-time, one gets

$$\frac{U^{n+1,m+1} - U^{n+1,m}}{\partial \tau} + I^m \left[\frac{3\left(U^{n+1,m+1} - U^n\right)}{2\Delta t} - \frac{\left(U^n - U^{n-1}\right)}{2\Delta t} \right] = \mathrm{Re}\, s^{n+1,m+1} \quad (6.71)$$

where U^n and U^{n-1} are frozen in pseudo iterations since there is no way of changing them. By a slight modification of the above equation some implicitness can be introduced into the pseudo iterations as

$$\frac{U^{n+1,m+1} - U^{n+1,m}}{\Delta \tau} = -I'_m \left[\frac{3\left(U^{n+1,m} - U^n\right)}{2\Delta t} - \frac{\left(U^n - U^{n-1}\right)}{2\Delta t} \right] + \mathrm{Re}\, s^{n+1,m+1} \quad (6.72)$$

where I is the unit matrix and $I'_m = \left[I + 1.5 \frac{\Delta \tau}{\Delta t} I_m \right]^{-1} I_m$ is the modified diagonal matrix.

By this way, the time derivative term was made explicit but the residual still requires the implicit treatment. To establish that, implicit time stepping or explicit RK time algorithm can be used. Although the implicit time stepping provides very quick convergence rates, it is very difficult to implement it here as discussed before. Instead, multi-stage RK algorithm given below was used to improve the residual for the next pseudo-time iteration:

$$U^{n+1,k+1} = U^{n+1,k} + \alpha^k \left[I + 1.5 \frac{\Delta \tau}{\Delta t} I_m \right]^{-1} \left[\mathrm{Re}\, s^{n+1,k+1} \right]^* \quad (6.73)$$

$$\left[\mathrm{Re}\, s^{n+1,k+1} \right]^* = \mathrm{Re}\, s^{n+1,k} - I_m \left[\frac{3\left(U^{n+1,k} - U^n\right)}{2\Delta t} - \frac{\left(U^n - U^{n-1}\right)}{2\Delta t} \right] \quad (6.74)$$

where k is the RK stage and α_k are the RK parameters. After RK steps are completed, one gets $U^{n+1,k+1} \rightarrow U^{n+1,m+1}$ and by the end of pseudo iterations, $\frac{\partial U}{\partial \tau} \rightarrow 0$ and thus

$U^{n+1,m+1} \rightarrow U^{n+1}$ recovering and obtaining the corrected solution at the new time level n+1. The numerical experience shows that the pseudo iterations usually converges within 5 to 10 iterations. Note that this implicit procedure is more accurate than the explicit treatment considered.

6.5. The Runga-Kutta Schemes

An important family of time-integration techniques which are of a high order of accuracy, explicit but non-linear, and limited to two time levels is provided by Runge-Kutta methods. Compared with the linear multi-step method the Runge-Kutta schemes achieve high orders of accuracy by sacrificing the linearity of the method but maintaining the advantages of the one-step method, while the former are basically of a linear nature but achieve great accuracy by involving multiple time steps. A detailed description of the Runge-Kutta method can be found in Gear (1971), Lambert (1974) and Van der Houwen (1977). These methods have recently been applied to the solution of Euler equations by Jameson *et al.* (1981) and further developed to highly efficient operational codes (Jameson and Baker, 1983, 1984).

The basic idea of the Runge-Kutta methods is to evaluate the right-hand side of the differential system at several values of U in the interval between $n \, \Delta t$ and $(n + 1) \, \Delta t$ and to combine them in order to obtain a high-order approximation of U^{n+1}. The general form of a *K-stage* Runge-Kutta method is as follows:

$$U^{(1)} = U^n$$

$$U^{(2)} = U^n + \Delta t \alpha_2 \, \mathrm{Re}\, s(U^{(1)})$$

$$U^{(3)} = U^n + \Delta t \alpha_3 \, \mathrm{Re}\, s\left(U^{(2)}\right) \tag{6.75}$$

$$\vdots$$

$$U^{(K)} = U^n + \Delta t \alpha_K \, \mathrm{Re}\, s\left(U^{(K-1)}\right)$$

Note that Equation (6.75) is not the most general form of the Runge-Kutta schemes, since Res is only a function of $U^{(k)}$. The most popular version is the fourth-order Runge-Kutta method, defined by the coefficients

$$\alpha_2 = \frac{1}{2} \quad \alpha_3 = \frac{1}{2} \quad \alpha_4 = 1$$

$$\beta_1 = \frac{1}{6} \quad \beta_2 = \beta_3 = \frac{1}{3} \quad \beta_4 = \frac{1}{6} \tag{6.76}$$

leading to (6.75)

$$U^{n+1} = U^n + \frac{\Delta t}{6}\left(\operatorname{Res}\left(U^n\right) + 2\operatorname{Res}\left(U^{(2)}\right) + 2\operatorname{Res}\left(U^{(3)}\right) + \operatorname{Res}\left(U^{(4)}\right)\right) \tag{6.77}$$

where $Res(U^{(1)})$ has been written as $\operatorname{Res}(U^n)$.

A well-known two-stage Runge-Kutta method (Heun's method) is defined by the predictor-corrector scheme. With the restriction to order two there exists an infinite number of two-stage Runge-Kutta methods with order two but none with an order higher than two. They all can be considered as predictor-corrector schemes Note that for each number of stages K there is an infinite number of possible Runge-Kutta schemes, with maximum order of accuracy. An even larger member of free parameters can be selected when the requirements on the order of accuracy are relaxed.

7. NUMERICAL RESULTS

This chapter presents two dimensional numerical results in order to show the capability and accuracy of the scheme introduced. First, NS solutions with no electric and magnetic fields are presented for steady state and unsteady (time dependent) problems. After showing the correctness and robustness of the code by means of these numerical results, a test problem in MHD (including *E and B fields*) will be presented.

7.1. The steady lid-driven cavity problem

The calculation of laminar incompressible driven flows in a square unit cavity whose top wall moves with a uniform velocity has often been used as a model problem for testing numerical techniques devoted to steady calculations. For low to moderately high values of the Reynolds number (based on the constant velocity of the upper wall: $Re = uL / v$), several results have been published using various solution procedures and different mesh sizes. A reference solution for steady flows is given in [11], where accurate calculations are performed for Reynolds numbers from 100-1000 in uniform meshes.

The present calculations have been done starting with an initial zero velocity field and using CFL = 2, β = 1. An example of isotropic mesh used for these calculations are shown in Figure7.1 for two different grid sizes:33x33 and 133x133.
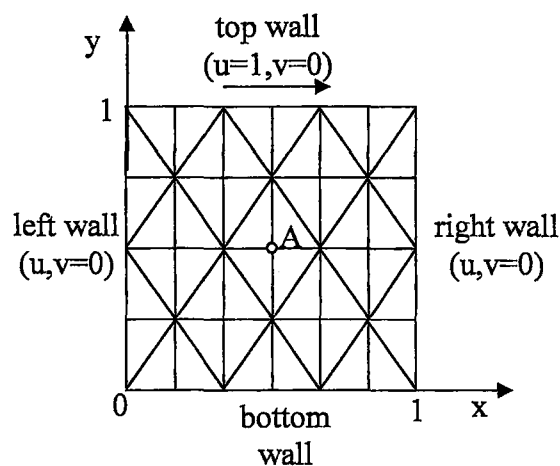

Figure 7.1. An example of square isotropic mesh used for the steady lid

The *u-velocity* profiles versus y at the geometric center (passing from point A on Figure.7.1) of the cavity (at $y = 0.5$) are presented in Figure 7.1 for Re = 100 and 400. In addition, the *v-velocity* profiles versus x at the geometric center of the cavity (at $x = 0.5$) are presented in Figure 7.1 for Re = 100 and 400.

Although higher Reynolds numbers usually require finer grid resolution as the viscous effect is concentrated very close to the wall, the results for Re=400 show that no such grid stretching is required. The u and v;-profiles, presented in Figures 7.2 and 7.3 show excellent agreement with the results given in [11].
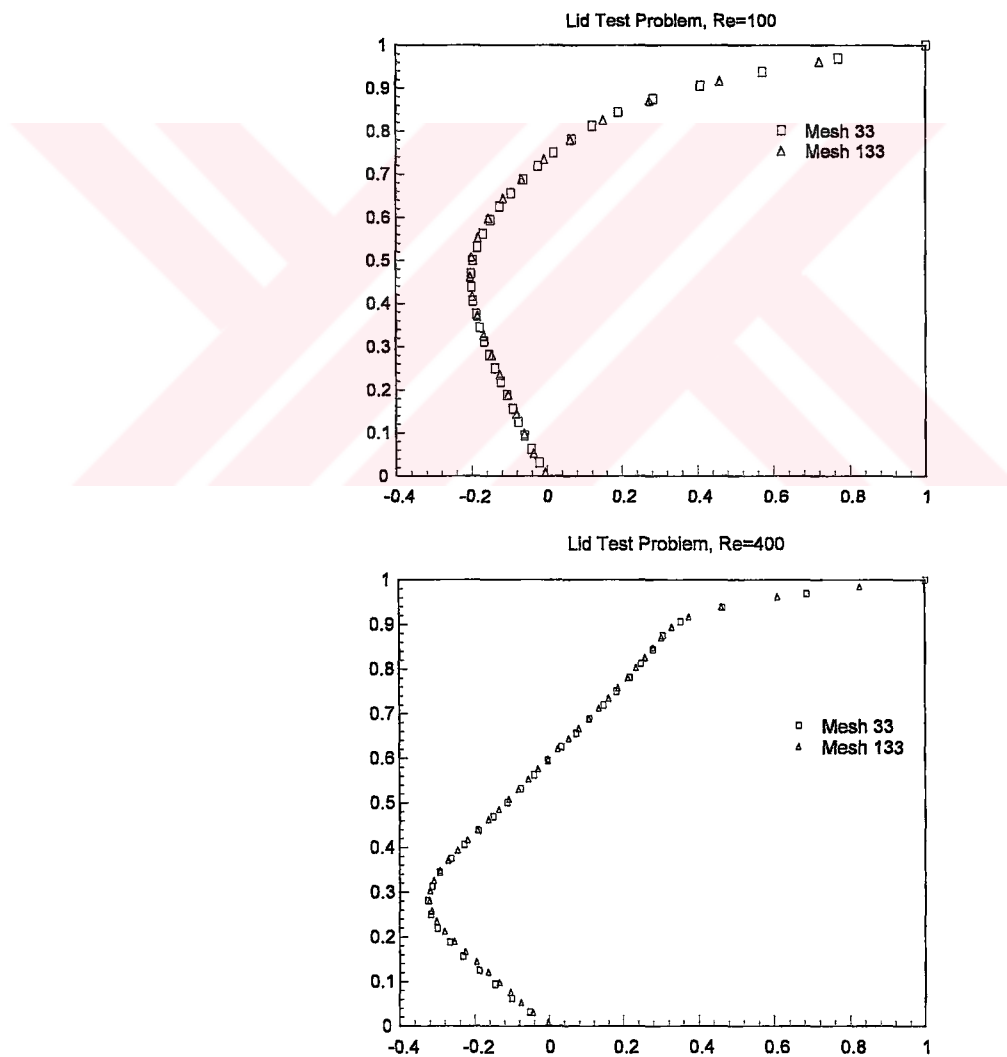
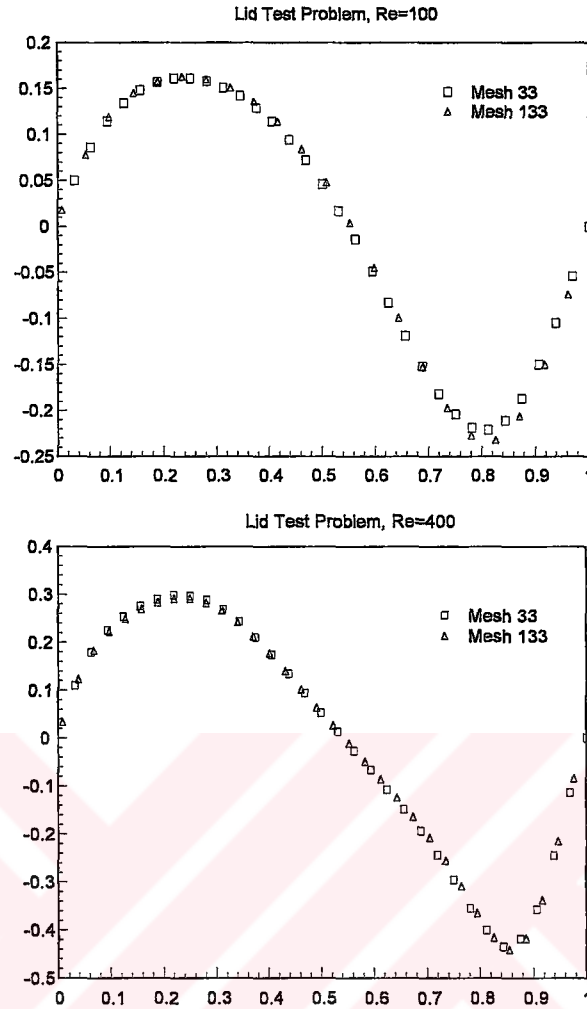Figure7.2. The"y" profile of "u" for the Lid test for *Re=100 and 400* at two different isotropic mesh.

Figure 7.3. The"x" profile of "v" for the Lid test for *Re=100 and 400* at two different isotropic mesh.

In order to have an idea of the convergence speed, we show in Figure 7.3 the convergence history (based on all the variables) for the different Re numbers and meshes. The residual drops by four orders of magnitude within 500 iterations and the steady state is achieved. We stop the calculations when the relative error (the maximum change in the state between two time levels). As seen, the convergence is quite rapid although no additional acceleration process, such as the multigrid technique is used here. This result shows that the code presented can be used to investigate the steady behaviour of flows.
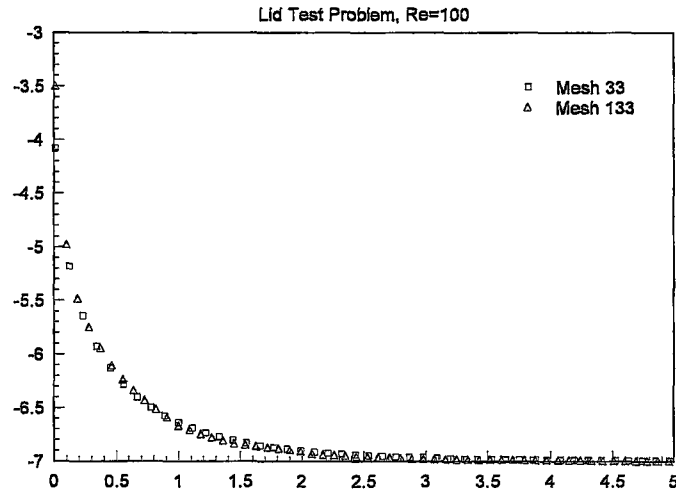
Figure7.4. The time history of residul for the Lid test for *Re=100* at two different isotropic mesh.

7.2. Unsteady lid-driven cavity problem

A review of the lid-driven cavity problem for steady and unsteady laminar "incompressible flows and numerous results were published by Gustafson and Halasi [14] for several cavity geometries.

In this test, an impulsively starting flow in a lid-driven cavity of aspect ratio $A = 1$ (square medium) is considered. The velocity of the moving lid is given by a step function defined by

$$\begin{cases} U_{lid} = 0 \ , \ \ t < 0 \\ U_{lid} = 1 \ , \ \ t \geq 0 \end{cases}$$ (7.1)

This problem was solved on the same mesh introduced in previous test and the time history of *u-velocity* at the center (see point A on Figure 7.1) was followed. For Re=400 and dt=0.025, the resulting time history is shown in Figure 7.5.

As seen from the figure, the coarse and fine mesh results match succesfully. Showing excellent agreement with [13], this result shows that the code can be used accurately for the time dependent (unsteady) problems.
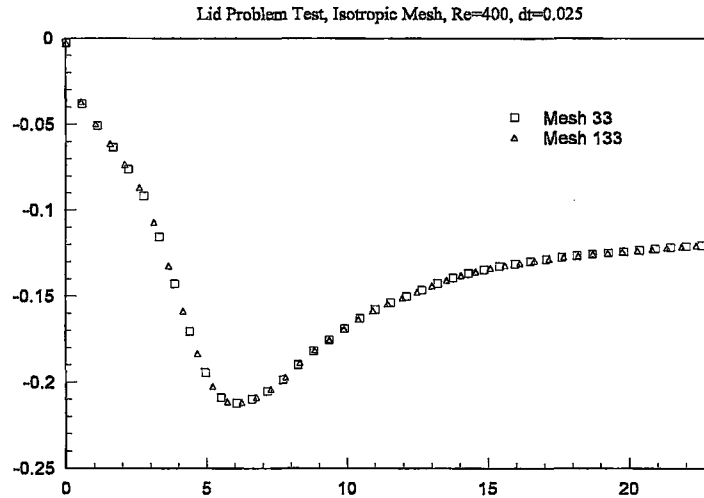

Figure7.5. The time history of the u velocity at the center of the cavity (the node at the center) for Re=400.

7.3. Unsteady Oscillatory lid-driven cavity problem

In this test case, we consider an oscillatory flow with of time-periodic lid velocity defined as $U_{lid}(t)=U_0 \cos t$. The Reynolds number is based on the maximum lid velocity U_0 and the aspect ratio A still equals one. In this test, the initial condition was taken to be zero velocity except the oscillating top velocity which starts from $U_{lid}(t)=1$ since $U_0=1$ was considered.

As time proceeds, sinusoidally changing lid velocity controls the flow inside the cavity and peridicity is achieved after nerly $t=5$. The drag at the top boundary was numerically calculated from

$$D = \int_0^1 \left[\frac{\partial u}{\partial y}\right]_{y=1} dx \cong \frac{3u_J - 4u_{J-1} + u_{J-2}}{2\Delta y}\Delta x \qquad (7.2)$$

where J is the index for the nodes at $y=1$ (the top boundary) and Δx and Δy are the x and y increments. This test problem was run on a square mesh shown in Figure 7.6 for $x,y \in [0,1]$

80

at two different grid resolution (i.e., 33x33 and 133x133, as done before). The resulting drag profile is shown in Figure 7.6. As seen the coarse and fine solutions agree and the time periodicity is achieved after t=5. These results agree very well with those presented in [14].
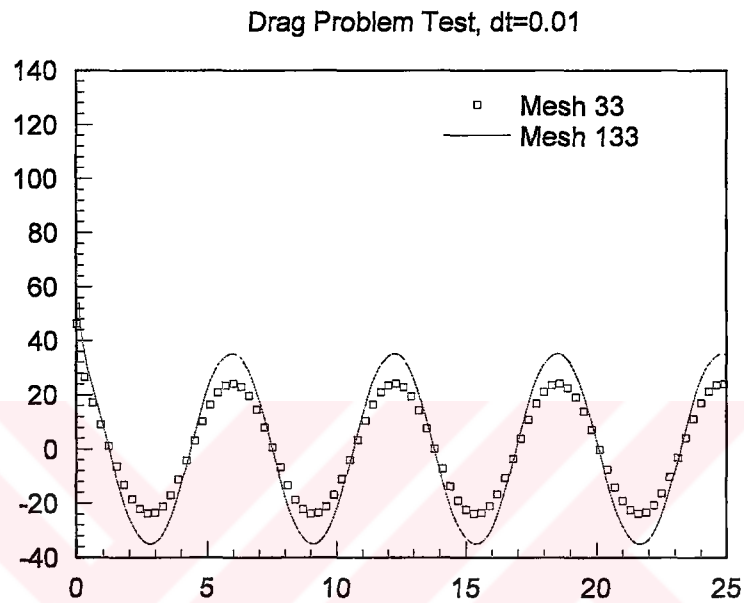

Figure7.6. The time history of the Drag at the top lid for Re=400.

7.4. Decaying Vortices

The temporal and spatial accuracy of the present numerical method is verified by simulating the following two-dimensional unsteady flow, which has been investigated by previous researchers:

$$u(x,y,t) = -\cos(\pi x)\sin(\pi y)e^{-2\pi^2 t/Re}$$

$$v(x,y,t) = \sin(\pi x)\cos(\pi y)e^{-2\pi^2 t/Re}$$

$$p(x,y,t) = -\frac{1}{4}(\cos 2\pi x + \cos 2\pi y)e^{-4\pi^2 t/Re}$$

The computational domain is $-1/2 < x, y < 1/2$ and computations are carried out at $Re = 10$, where $\text{Re} = U_1 L/\nu$ and U_1 is the initial maximum velocity and L is the size of a vortex. The initial velocity condition at $t = 0$ and the velocities at the boundaries in time are provided from the exact solution. Four different sizes of uniformly-distributed right-angled triangles are used to determine the overall accuracy of the present numerical method: numbers of cells used are 200, 800, 3200, and 12800, respectively. In this study, with mesh refinement, each triangle is split into four right-angled triangles as shown in Figure 7.1.

First, computations are performed with varying the mesh size but keeping the maximum CFL number constant. Figure 7.2 shows the variation of the maximum error in u with mesh refinement and the effect of the second term in Equation (7.2) on the overall accuracy for three different maximum CFL numbers. It is clear that the present numerical method including the second term in Equation (7.2) is second-order accurate for all the CFL numbers investigated. However, when the term is neglected, the error becomes larger and the accuracy is not second order. Note that the accuracy without the second term in Equation (7.2) becomes nearly a second order with CFL = 3 because the spatial-interpolation error contributes less to total error as the CFL (time step) increases. The same result is also obtained for ν.

Second, the spatial and temporal accuracies are investigated, respectively. Figure 7.2 shows the variation of the maximum error in u by varying mesh size but keeping the computational time step constant and therefore the slope shown in Figure 7.2 denotes the spatial accuracy. Note that the computational time step in this case is determined to be a small value ($\Delta t = 0.001$) such that temporal error has negligible effect on total error. It is clear that inclusion of the second term in Equation (7.2) makes the spatial accuracy second-order. Similarly, the temporal accuracy is investigated by varying the time step but keeping the mesh size constant. Here, the finest grid of 12800 cells is used to minimize the spatial error. Figure 7.2 shows that the present time integration scheme is indeed second-order accurate.

7.4. The natural flow in cavity by different wall temperatures

This test case presents the temperature variation in a square cavity whose walls are kept at two different temperatures. The buoyancy effects drives natural flow along the walls and creates circulation in the cavity. The boundary conditions and the example of the mesh (64x64 isotropic mesh) used is shown in Figure 7.7.
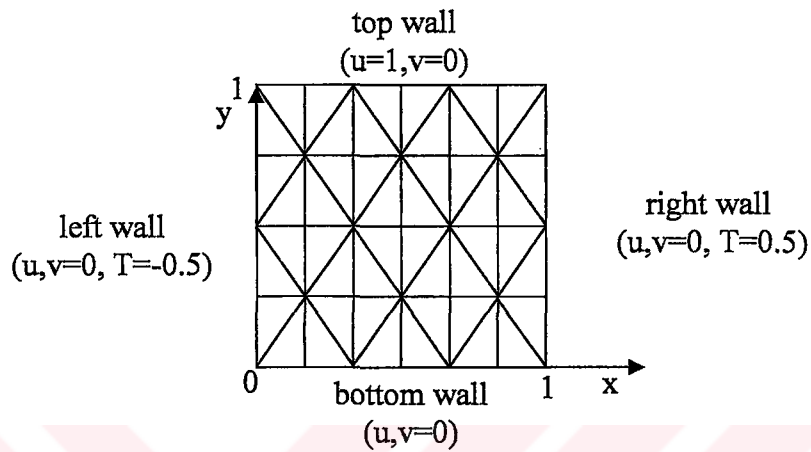

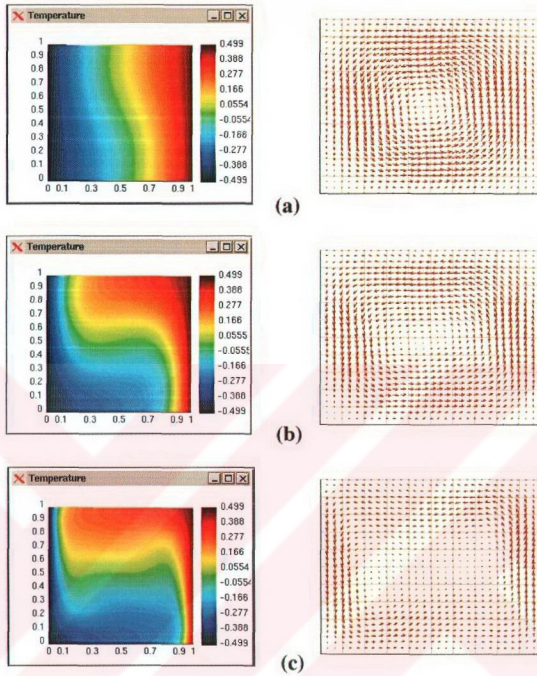Figure7.7. The temperature profiles in cavity for Re=400 and Ra=1000, 10000, and 100000.

Figure7.8. The temperature profiles in cavity for Re=400 and Ra=1000, 10000, and 100000.

7.5. Electromagnetic Breaking Test

This test case presents the slowing down of vertical flow of liquid metals through pipes by means of externally applied electric and magnetic fields. The flow and system structure is shown in Figure 7.9. As seen from this figure, the flow which is downward through the rectangular pipe is slowed down by applying an external force (**ExB** force) opposite to the gravitational force in $-y$ direction.
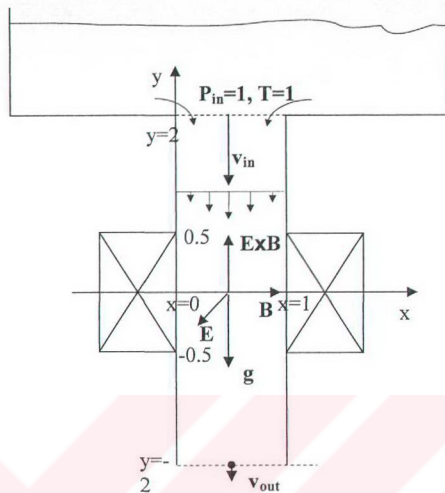
Figure7.9 Electromagnetic brake system by using **B** and **E** fields. **ExB** force is opposite to the gravitational force.

The external magnetic field (which is directed in +x direction) is created by the magnets placed on both sides of the channel. The electric field is produced by charging two plates and placing them along the +z direction. Figure 7.9 shows this configuration. Since external magnetic field contribution sould be found by solving the steady-state Maxwell's equations (i.e., $\nabla \cdot B_{ext} = 0$, $\nabla \times B_{ext} = 0$) and carefully chosen boundary conditions. The electric and magnetic field are activated by using a switch and opening this switch some time after the steady vertical flow is established. Figure 7.10 shows the resulting magnetic field configuration and the temperature increase because of the external field region along the channel.
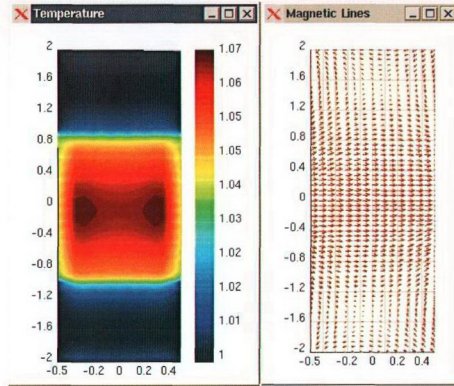
Figure7.10. The external magnetic and electric field configuration and the temperature increase along the channel.

The purpose of this study is to find out if there is a slow down in the vertical velocity when the strength of externally applied electric is increased. This is done by choosing a point (at which the vertical velocity is maximum) at the exit of the channel and following the vertical velocity at that point as a function of time for different values of external electric field. This result is shown in Figure 7.11. As seen, the results fulfill the physical expectations since the magnitude of the vertical flow reduces as the strength of the external electric field is increased.
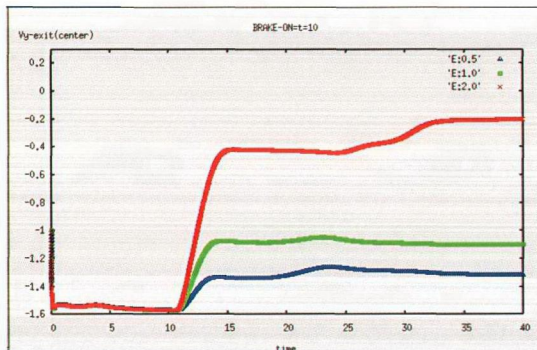

Figure7.11. The effect of external electric field strength on the vertical velocity measured at the centerline at the exit of the channel.

8. CONCLUSION

This thesis is about the laminar flows through cavities and channels. The laminar flows in channels were investigated by the solutions of Navier-Stokes (N-S) equations. The numerical method was developed by using a matrix distribution scheme that operates on the structured or unstructured triangular meshes. The time advancement was established by using a dual time stepping scheme in which pseudo time iterations causes a relaxation scheme to drive the divergence of the velocity reduces to a lower value before advancement to the new time level. The Navier-Stokes equations and the equations describing the electromagnetic field (MHD) were solved in order to investigate two-dimensional flows on x-y plane. The external electric and magnetic fields are applied in perpendicular direction such that **ExB** becomes opposite to gravitational acceleration direction so that the vertical velocity is slowed down the channel. The numerical results show that this computer code is capable of resolving different types of problems in different geometries.

REFERENCES

1. CHEN, *Introduction To Plasma physics & Controlled Fusion,* Second Edition 1 Plenum, 2002.

2. HIRSCH, *Numerical Computation of Internal & Enternal Flows* Volume 1, 2001.

3. Granger, *Fluid Mechanics,*1999.

4. Bertin Smith, *Aerodynamics For Engineers,1998.*

5. I. G. CURRIE, *Fundamental Mechanics of Fluids, 1997.*

6. Victor L., E. Benjamin, Keith W., Streeter Wylie Bedford, *Fluid Mechanics* (9th Edition), , WCB/Mc Graw Hill, 1998.

7. Nakayama, *PC-Aided Numerical heat Transfer and Convective Flow*, 2000.

8. R. V. Polovin and V. P. Demutskii, *Fundamentals of Magnetohydrodynamics, 1996.*

9. Lyle D. Dailey and Richard H. Pletcher, *Evaluation of multigrid acceleration for preconditioned time-accurate navier-stokes algorithms,* 1996.
.

10. E. van der Weide & H. Deconinck, *Matrix distribution schemes for the system of euler equations,* 1996.

11. Roland W. Lewis, Perumal Nithiarasu, Kankanhalli N. Seetharamu, *Fundamentals of the Finite Element Method for heat and Fluid Flow, 1998.*

12. I. G. Currie, *Fundamental mechanics of fluids, 2001.*

13. Dongjoo Kim and Haecheon Choi, *A second-Order Time-Accurate Finite Volume method for Unsteady Incompressible Flow on Hybrid Unstructured Grids,* 1999-2000.

14. Benoit Granier, Alain Lerat and Zi-Niu Wu, *An implicit centered scheme for steady and unsteady incompressible one and two-phase flows,* 1995-1996.

15. T.C. Warburton and G. e. Karniadakis, *A discontinuos Galerkin Method for the viscous MHD Equations,* 1998-1999.

16. Dongjoo Kim and Haecheon Choi, *A second-order time-accurate finite volume method for unsteady incompressible flow on hybrid unstructured grids,* 1999-2000.

17. M. Hughes, K. a. Pericleous and M. Cross, *The numerical modeling of DC electromagnetic pump and brake flow, 1999.*

18. D. Gao, N. B. Morley, V. Dhir, *Numerical study of liquid metal film flows in a varying spanwise magnetic field,* 1998-1999.

19. Takehiko Sato, Oleg P. Solonenko, Hideya Nishiyama, *Numerical simulation of a particle-laden plasma flow in a complex configuration under an electromagnetic field,* 2001-2002.

20. Asuncion V. Lemoff, Abraham P. Lee, *An AC magnetohydrodynamic micropump,* 2001.

21. F. Armero, J. C. Simo, *Long-term dissipativity of time-stepping algorithms for an abstract evolution equation with applications to the incompressible MHD and Navier-Stokes equations,* 1994-1995.

REFERENCES NOT CITED

E. van der Weide and H. Deconinck von Karman Institute for Fluid Dynamics, *Matrix Distribution Schemes for the system of Euler Equations, 1998.*

Necdet Aslan, *A visual fluctuation splitting scheme for magnetohydrodynamics with a new sonic fix and Euler limit,* 2003-2004.

Necdet Aslan, *A visual unsteady navier stokes solver with radiation, mass, and heat transfer,* 2002.

Amnon J. Meir, Sayavur I. Bakhtiyarov, Paul G. Schmidt, Ruel A. Overfelt, V*elocity, potential, and temperature distributions in molten metals during electromagnetic stirring. Part II. Numerical simulations, 2001.*

Necdet Aslan, *Ainss-1: An incompressible navier-stokes solver on structured and unstructured triangular meshes,* 2000.

Benoit Granier, Alain Lerat and Zi-Niu Wu, *An implicit centered scheme for steady and unsteady incompressible one and two-phase flows,* 1995-1996.

Mao-Chung Hsieh, Ing-Jer Lin, and Jinn-Liang Liu, *An adaptive least squares finite element method for navier-stokes equations, 2000.*